MATHEMATICS OF COMPUTATION

Volume 93, Number 349, September 2024, Pages 2185–2214 https://doi.org/10.1090/mcom/3916 Article electronically published on November 20, 2023

CONVERGENCE ANALYSIS OF A POSITIVITY-PRESERVING NUMERICAL SCHEME FOR THE CAHN-HILLIARD-STOKES SYSTEM WITH FLORY-HUGGINS ENERGY POTENTIAL

YUNZHUO GUO, CHENG WANG, STEVEN M. WISE, AND ZHENGRU ZHANG

Abstract. A finite difference numerical scheme is proposed and analyzed for the Cahn-Hilliard-Stokes system with Flory-Huggins energy functional. A convex splitting is applied to the chemical potential, which in turns leads to the implicit treatment for the singular logarithmic terms and the surface diffusion term, and an explicit update for the expansive concave term. The convective term for the phase variable, as well as the coupled term in the Stokes equation, is approximated in a semi-implicit manner. In the spatial discretization, the marker and cell difference method is applied, which evaluates the velocity components, the pressure and the phase variable at different cell locations. Such an approach ensures the divergence-free feature of the discrete velocity, and this property plays an important role in the analysis. The positivity-preserving property and the unique solvability of the proposed numerical scheme are theoretically justified, utilizing the singular nature of the logarithmic term as the phase variable approaches the singular limit values. An unconditional energy stability analysis is standard, as an outcome of the convex-concave decomposition technique. A convergence analysis with accompanying error estimate is provided for the proposed numerical scheme. In particular, a higher order consistency analysis, accomplished by supplementary functions, is performed to ensure the separation properties of numerical solution. In turn, using the approach of rough and refined error estimates, we are able to derive an optimal rate convergence. To conclude, several numerical experiments are presented to validate the theoretical analysis.

1. Introduction

The Cahn-Hilliard-Stokes (CHS) system, a gradient flow equation coupled with incompressible fluid motion, can be used to describe the phase separation and flow of a very viscous binary fluid Π . Let $\Omega \in \mathbb{R}^d$, d = 2, 3, be an open domain. The

©2023 American Mathematical Society

Received by the editor March 20, 2023, and, in revised form, August 15, 2023, and September 17, 2023.

²⁰²⁰ Mathematics Subject Classification. Primary 35K35, 35K55, 49J40, 65M06, 65M12.

Key words and phrases. Cahn-Hilliard-Stokes system, logarithmic energy potential, convex splitting, positivity-preserving, energy stability, optimal rate convergence analysis.

The second author was partially supported by the NSF DMS-2012269, DMS-2309548. The third author was partially supported by the NSF DMS-2012634, DMS-2309547. The fourth author was partially supported by the NSFC No. 11871105 and Science Challenge Project No. TZ2018002.

The second author is the corresponding author.

following CHS system with Flory-Huggins potential is considered:

(1.1)
$$\partial_t \phi + \nabla \cdot (\phi \mathbf{u}) = \Delta \mu,$$

(1.2)
$$-\Delta \boldsymbol{u} + \boldsymbol{u} = -\nabla p - \gamma \phi \nabla \mu,$$

$$(1.3) \nabla \cdot \boldsymbol{u} = 0,$$

(1.4)
$$\mu = \delta_{\phi} E = \ln(1+\phi) - \ln(1-\phi) - \theta_0 \phi - \varepsilon^2 \Delta \phi,$$

with no-flux and no-penetration free-slip boundary conditions,

(1.5)
$$\partial_n \phi = \partial_n \mu = 0, \quad \boldsymbol{u} \cdot \boldsymbol{n} = \partial_n (\boldsymbol{u} \cdot \boldsymbol{\tau}) = 0 \quad \text{on } \partial\Omega \times (0, T].$$

In this system, ϕ is a binary fluid concentration, μ , p and u describe the chemical potential, pressure and fluid velocity vector, respectively. The parameter $\gamma > 0$ is related to surface tension. Observe that equations (I.1)–(I.4) correspond to a simplified version of a model studied by others, obtained by assuming that two fluids have the same densities, and the gravity effects may be ignored [10,25].

For the fluid part of the physical system, the no-penetration boundary condition, $\boldsymbol{u}\cdot\boldsymbol{n}=0$ on $\partial\Omega$, is natural. Meanwhile, both the no-slip boundary condition, $\boldsymbol{u}\cdot\boldsymbol{\tau}=0$, and free-slip boundary condition, $\partial_n(\boldsymbol{u}\cdot\boldsymbol{\tau})=0$ (on $\partial\Omega$), are physically reasonable. On the other hand, the Stokes operator with the free-slip boundary condition is symmetric, due to the homogeneous Neumann boundary condition for the pressure field induced by this boundary condition. As a result, the analysis with free-slip boundary condition becomes simpler than the one with no-slip boundary condition. For simplicity of presentation, we only focus on the free-slip boundary condition for the velocity vector in this article, although the analysis could be similarly extended to the one with no-slip boundary condition; the technical details are left to interested readers.

For any $\phi \in H^1(\Omega)$, with the point-wise bound $-1 < \phi < 1$, the Flory-Huggins free energy functional is given by

(1.6)
$$F(\phi) = \int_{\Omega} \left((1+\phi) \ln(1+\phi) + (1-\phi) \ln(1-\phi) - \frac{\theta_0}{2} \phi^2 + \frac{\varepsilon^2}{2} |\nabla \phi|^2 \right) d\mathbf{x},$$

in which ε , θ_0 are positive constants associated with the diffuse interface width. The following dissipation property is valid for the energy functional (1.6):

(1.7)
$$\partial_t F(\phi) = -\|\nabla \mu\|^2 - \frac{1}{\gamma} \left(\|u\|^2 + \|\nabla u\|^2 \right).$$

It is clear that the logarithmic free energy functional has a singularity near the values of ± 1 , which poses a great challenge in the numerical design. As an alternate approach, a nonsingular polynomial energy has also been widely used

(1.8)
$$F(\phi) = \int_{\Omega} \left(\frac{1}{4} \left(\phi^2 - 1 \right)^2 + \frac{\varepsilon^2}{2} |\nabla \phi|^2 \right) d\mathbf{x}.$$

Similar to (1.6), this model has a double-well potential, which can be regarded as a polynomial approximation to the original one, with a larger error in the actual physical situation [2]. A finite element analysis of (1.1)—(1.2), with an added time derivative in the Stokes equation and polynomial energy (1.8), was reported in a recent paper [11].

One can show that, for these particular flow boundary conditions, if the fields are sufficiently regular, it follows that

(1.9)
$$-\Delta p = \gamma \nabla \cdot (\phi \nabla \mu) \quad \text{in } \Omega,$$

$$(1.10) -\partial_n p = \gamma \phi \partial_n \mu = 0 \text{on } \partial \Omega.$$

In short, one can separate the pressure and velocity calculations. Taking advantage of this property, let us define a Helmholtz-type projection as follows:

(1.11)
$$\mathcal{P}_{H}: \left\{ \boldsymbol{f} \in \left[H^{1}(\Omega)\right]^{3} \mid \boldsymbol{f} \cdot \boldsymbol{n} = 0 \text{ on } \partial\Omega \right\} \\ \rightarrow \left\{ \boldsymbol{v} \in \left[H^{1}(\Omega)\right]^{3} \mid \nabla \cdot \boldsymbol{v} = 0 \text{ in } \Omega, \ \boldsymbol{v} \cdot \boldsymbol{n} = 0 \text{ on } \partial\Omega \right\},$$

where $\mathcal{P}_H(\boldsymbol{f}) := \boldsymbol{f} + \nabla p$, where $p \in \mathring{H}^2_N(\Omega) \cap H^1(\Omega)$ is the unique solution to $-\Delta p = \nabla \cdot \boldsymbol{f}$ in Ω , as in (1.9)–(1.10). Here

$$\begin{split} H^2_N(\Omega) &:= \left\{ \phi \in H^2(\Omega) \; \middle| \; \partial_n \phi = 0 \text{ on } \partial \Omega \; \right\} \quad \text{and} \\ \mathring{H}^2_N(\Omega) &:= \left\{ \phi \in H^2_N(\Omega) \; \middle| \; (\phi, 1) = 0 \right\}. \end{split}$$

Clearly,

$$(\mathcal{P}_H(\boldsymbol{f}), \boldsymbol{f} - \mathcal{P}_H(\boldsymbol{f}))_{L^2} = 0.$$

From this we can prove the L^2 stability of the projection. Of course, sufficiently regular solutions to the CHS system (1.1)–(1.4) satisfy

$$-\Delta \boldsymbol{u} + \boldsymbol{u} = -\gamma \mathcal{P}_H \left(\phi \nabla \mu \right),$$

assuming the no flux, no-penetration, and free-slip boundary conditions. Thus, the Cahn-Hilliard-Stokes system can be reformulated to, effectively, remove the velocity:

(1.12)
$$\begin{aligned} \phi_t + \nabla \cdot (\boldsymbol{u}\phi) &= \Delta \mu, \\ \boldsymbol{u} &= -\mathcal{S}^{-1} \mathcal{P}_H \gamma(\phi \nabla \mu), \end{aligned}$$

where

$$S := -\Delta + I$$
,

with the appropriate boundary conditions. One can observe that equation (1.12) is, in essence, a Cahn-Hilliard-type equation, a modified gradient flow.

For this PDE system, a positivity-preserving property, that is, $1 + \phi > 0$ and $1 - \phi > 0$, can be theoretically justified, due to the logarithmic terms appearing in μ . Of course, the numerical analysis of the Cahn-Hilliard equation, by itself, is an interesting topic, and recent works have been devoted to that equation with an assumed Flory-Huggins potential: for example, the finite difference method 2 and the finite element approach 1,38.

The question of energy stability has always been an essential issue for any numerical approximation to a gradient flow coupled with fluid motion, and some existing works have been reported [12,23,34]. Meanwhile, most existing numerical efforts have been based on the polynomial approximation in the energy potential, so that singularities can be avoided with respect to the phase variable. For the Flory-Huggins energy potential (1.6) and the corresponding CHS system (1.1)—(1.4), the preservation of both the point-wise positivity (for the logarithmic arguments) and the energy stability turns out to be a very challenging issue. This comes from the highly nonlinear, singular, and coupled nature of the PDE system. In this work, a fully discrete finite difference scheme is proposed and analyzed for solving the

CHS system with logarithmic Flory-Huggins potential. Four theoretical properties will be justified for the numerical scheme: positivity-preserving, unique solvability, unconditional energy stability (in the physical free energy), and optimal rate convergence.

In more details, the numerical approximation to the chemical potential is based on the convex-concave decomposition of the Flory-Huggins energy functional, which dates back to Eyre [19]. This approach ensures a theoretical justification of its positivity-preserving property, because of an implicit treatment of the nonlinear singular logarithmic term. In particular, the singular and convex nature of the logarithmic term prevents the numerical solution reaching the singular limit values, so that a point-wise positivity is preserved for the phase variable. See the related works 6.8.13-15.17,28-30,32,39,40 of the positivity-preserving analysis for various gradient flow models with singular energy potential. The linear expansive term is explicitly updated, for the sake of unique solvability, due to the negative eigenvalues involved. The surface diffusion term is implicitly treated, which comes from its convexity. Meanwhile, the other parts of the CHS system have to be handled very carefully, to ensure the desired theoretical properties. The convective term in the phase field dynamic equation is discretized in a semi-implicit way: explicit treatment for the phase variable and implicit treatment for the velocity vector. The static Stokes equation is implicitly computed, with the chemical potential determined by the convex splitting approach. The full numerical system turns out to be the gradient of a strictly convex energy functional, which in turn guarantees the unique solvability of the numerical solution. This symmetric feature represents a key difference between the current work and the related works in 45, in which the discretization of the Cahn-Hilliard-Navier-Stokes system leads to a nonsymmetric numerical system, due to the fluid convection terms. As a result of the unique solvability and positivity-preserving property, the energy dissipation of the numerical scheme could be derived by a standard energy estimate.

In the present paper, an optimal rate convergence analysis and error estimate of the proposed numerical scheme are provided, which will be the first such result for the singular energy potential phase field model coupled with fluid motion. As illustrated by a few related existing works [2,3,7,12,31] for the fluid-phase field coupled system with a polynomial approximation energy potential, the standard $\ell^{\infty}(0,T;\ell^2)\cap\ell^2(0,T;H_h^2)$ error estimate does not work for the CHS system (L.1)–(L.4), due to the lack of control for the highly nonlinear convection term. Instead, we have to perform an $\ell^{\infty}(0,T;H_h^1)\cap\ell^2(0,T;H_h^3)$ error estimate, and such an estimate in a higher order Sobolev norm is necessary to make the error term associated with the nonlinear convection term have a nonpositive inner product with the appropriate error test function.

In addition to the positivity-preserving property, the separation property of the numerical solution, i.e., a uniform distance between the numerical solution and the singular limit values (-1 and 1) is needed in the nonlinear error estimate. However, such a uniform bound is not directly available in any global-in-time analysis. To overcome this difficulty, a combination of rough and refined error (RRE) estimates must be applied. This RRE technique has been successfully applied to various nonlinear PDEs [16-18,[26,[27,[29]]]. In more details, a higher order asymptotic expansion, up to the second order temporal accuracy, is performed with a careful linearization technique. Such a higher order asymptotic expansion enables one to obtain a rough

error estimate, so that the ℓ^{∞} bound for the phase variable could be derived. This bound then plays a crucial role in the subsequent analysis. Namely, the refined error estimate is carried out to accomplish the desired convergence result.

The rest of the paper is organized as follows. In Section 2 the standard finite difference spatial approximation is recalled. In Section 3 we propose the fully discrete finite difference scheme and establish the positivity-preserving property, unique solvability and unconditional energy stability. The convergence analysis of the numerical scheme, with first order temporal accuracy and second order spatial accuracy, is provided in Section 5 Some numerical experiments are presented in Section 5 Finally, some concluding remarks are given in Section 6

2. The spatial discretization

The standard centered finite difference spatial approximation is applied. We present the numerical approximation on the computational domain $\Omega=(0,L_x)\times(0,L_y)\times(0,L_z)$. The notation of two-dimensional domain could be naturally extended. More relevant details and descriptions can be found in the related reference works [7,24,33,37].

2.1. **Basic definitions.** For simplicity, we consider $\Omega = (0, L_x) \times (0, L_y) \times (0, L_z)$, and assume that $h = L_x/N_x = L_y/N_y = L_z/N_z$, where h is the spatial size, and N_x , N_y , N_z are given integers. We define the following:

Definition 2.1. For any positive integer N, the following point sets are defined:

$$E_N := \{i \cdot h | i = 0, \dots, N\}, \quad C_N := \{(i - 1/2) \cdot h | i = 1, \dots, N\},$$

 $C_{\bar{N}} := \{(i - 1/2) \cdot h | i = 0, \dots, N + 1\}.$

The two points belonging to $C_{\bar{N}} \setminus C_N$ are the so-called ghost points. Define the function spaces

$$\mathcal{C}_{\Omega} := \{ \phi : C_{\bar{N}_x} \times C_{\bar{N}_y} \times C_{\bar{N}_z} \to \mathbb{R} \},$$

$$\mathcal{E}_{\Omega}^x := \{ \phi : E_{N_x} \times C_{N_y} \times C_{N_z} \to \mathbb{R} \}, \quad \mathcal{E}_{\Omega}^y := \{ \phi : C_{N_x} \times E_{N_y} \times E_{N_z} \to \mathbb{R} \}.$$

$$\mathcal{E}_{\Omega}^z := \{ \phi : C_{N_x} \times C_{N_y} \times E_{N_z} \to \mathbb{R} \}, \quad \mathcal{E}_{\Omega} := \mathcal{E}_{\Omega}^x \times \mathcal{E}_{\Omega}^y \times \mathcal{E}_{\Omega}^z.$$

The functions of \mathcal{C}_{Ω} are called cell-centered functions. In the component form, cell-centered functions are identified via $\phi_{i,j,k} := \phi(\xi_i, \xi_j, \xi_k)$, where $\xi_i := (i - \frac{1}{2}) \cdot h$. The functions of \mathcal{E}_{Ω}^x , etc., are called face-centered functions. In the component form, face-centered functions are identified via $f_{i+\frac{1}{2},j,k} := f(\xi_{i+\frac{1}{2}}, \xi_j, \xi_k)$, etc.

The discrete boundary conditions, associated with cell-centered function and edge-centered function, respectively, are proposed in Definition [2.2].

Definition 2.2. A discrete function $\phi \in \mathcal{C}_{\Omega}$ is said to satisfy homogeneous Neumann boundary conditions, and we write $\mathbf{n} \cdot \nabla_h \phi = 0$, iff ϕ satisfies

$$\phi_{0,j,k} = \phi_{1,j,k}, \qquad \phi_{N_x,j,k} = \phi_{N_x+1,j,k},
\phi_{i,0,k} = \phi_{i,1,k}, \qquad \phi_{i,N_y,k} = \phi_{i,N_y+1,k},
\phi_{i,j,0} = \phi_{i,j,0}, \qquad \phi_{i,j,N_x} = \phi_{i,j,N_x+1}.$$

A discrete function $\mathbf{f} = (f^x, f^y, f^z)^T \in \mathcal{E}_{\Omega}$ is said to satisfy no-penetration boundary conditions, $n \cdot f = 0$, iff we have

$$\begin{split} f^x_{1/2,j,k} &= 0, \qquad f^x_{N_x+1/2,j,k} &= 0, \\ f^y_{i,1/2,k} &= 0, \qquad f^y_{i,N_y+1/2,k} &= 0, \\ f^z_{i,j,1/2} &= 0, \qquad f^z_{i,j,N_k+1/2} &= 0. \end{split}$$

Definition 2.3. A discrete function $f = (f^x, f^y, f^z)^T \in \mathcal{E}_{\Omega}$ is said to satisfy free-slip boundary conditions iff we have

$$\begin{split} f^x_{i+1/2,0,k} &= f^x_{i+1/2,1,k}, & f^x_{i+1/2,N_y+1,k} &= f^x_{i+1/2,N_y,k}, \\ f^x_{i+1/2,j,0} &= f^x_{i+1/2,j,1}, & f^x_{i+1/2,j,N_z+1} &= f^x_{i+1/2,j,N_z}, \\ f^y_{0,j+1/2,k} &= f^y_{1,j+1/2,k}, & f^y_{N_x+1,j+1/2,k} &= f^y_{N_x,j+1/2,k}, \\ f^y_{i,j+1/2,0} &= f^y_{i,j+1/2,1}, & f^y_{i,j+1/2,N_z+1} &= f^y_{i,j+1/2,N_z}, \\ f^z_{0,j,k+1/2} &= f^z_{1,j,k+1/2}, & f^z_{N_x+1,j,k+1/2} &= f^z_{N_x,j,k+1/2}, \\ f^z_{i,0,k+1/2} &= f^z_{i,1,k+1/2}, & f^z_{i,N_y+1,k+1/2} &= f^z_{i,N_y,k+1/2}. \end{split}$$

The two-dimensional notation is similar:

$$\begin{split} f^x_{i+1/2,0} &= f^x_{i+1/2,1}, \qquad f^x_{i+1/2,N_y+1} = f^x_{i+1/2,N_y}, \\ f^y_{0,j+1/2} &= f^y_{1,j+1/2}, \qquad f^y_{N_x+1,j+1/2} = f^y_{N_x,j+1/2}. \end{split}$$

2.2. Discrete operators, inner products, and norms. The standard center difference operators are defined as follows:

Definition 2.4. Define $d_x: \mathcal{E}_{\Omega}^x \to \mathcal{C}_{\Omega}$ component-wise via

$$d_x f_{i,j,k} := \frac{1}{h} \left(f_{i+\frac{1}{2},j,k} - f_{i-\frac{1}{2},j,k} \right),$$

with $d_y:\mathcal{E}_{\Omega}^y\to\mathcal{C}_{\Omega}$ and $d_z:\mathcal{E}_{\Omega}^z\to\mathcal{C}_{\Omega}$ defined analogously. Then we have the discrete divergence:

$$\nabla_h \cdot : \mathcal{E}_{\Omega} \to \mathcal{C}_{\Omega}, \qquad \nabla_h \cdot \boldsymbol{f} := d_x f^x + d_y f^y + d_z f^z,$$

where $\boldsymbol{f} = (f^x, f^y, f^z)^T \in \mathcal{E}_{\Omega}$. Define $A_x : \mathcal{C}_{\Omega} \to \mathcal{E}_{\Omega}^x$ component-wise via

$$A_x \phi_{i+\frac{1}{2},j,k} := \frac{1}{2} \left(\phi_{i+1,j,k} + \phi_{i,j,k} \right),$$

while $A_y:\mathcal{C}_\Omega\to\mathcal{E}_\Omega^y$ and $A_z:\mathcal{C}_\Omega\to\mathcal{E}_\Omega^z$ could be analogously introduced. Then we have a discrete average:

$$A_h: \mathcal{C}_{\Omega} \to \mathcal{E}_{\Omega}, \quad A_h \phi := (A_x \phi, A_y \phi, A_z \phi)^T.$$

We define $D_x: \mathcal{C}_{\Omega} \to \mathcal{E}_{\Omega}^x$ component-wise via

$$D_x \phi_{i+\frac{1}{2},j,k} := \frac{1}{h} (\phi_{i+1,j,k} - \phi_{i,j,k}),$$

while $D_y:\mathcal{C}_\Omega\to\mathcal{E}_\Omega^y$ and $D_z:\mathcal{C}_\Omega\to\mathcal{E}_\Omega^z$ could be similarly introduced. The discrete gradient becomes

$$\nabla_h : \mathcal{C}_{\Omega} \to \mathcal{E}_{\Omega}, \qquad \nabla_h \phi := (D_x \phi, D_y \phi, D_z \phi)^T.$$

The standard discrete Laplace operator is defined as

$$\Delta_h: \mathcal{C}_{\Omega} \to \mathcal{C}_{\Omega}, \qquad \Delta_h \phi := \nabla_h \cdot \nabla_h \phi.$$

Remark 2.1. We can also define, in a straightforward way, the discrete Laplacian for face centered functions, $\Delta_h \mathcal{E}_{\Omega}^x \to \mathcal{E}_{\Omega}^x$, et cetera. For instance, if $g \in \mathcal{E}_{\Omega}^x$, then

$$\begin{split} & \Delta_h g_{i+\frac{1}{2},j,k} \\ & = \frac{g_{i+\frac{3}{2},j,k} + g_{i-\frac{1}{2},j,k} + g_{i+\frac{1}{2},j+1,k} + g_{i+\frac{1}{2},j-1,k} + g_{i+\frac{1}{2},j,k+1} + g_{i+\frac{1}{2},j,k-1} - 6g_{i+\frac{1}{2},j,k}}{h^2}, \end{split}$$

and likewise for functions in \mathcal{E}_{Ω}^{y} and \mathcal{E}_{Ω}^{z} .

Now we are ready to introduce the following grid inner products and norms.

Definition 2.5. Define

$$(\phi, \psi) := h^3 \sum_{i=1}^{N_x} \sum_{j=1}^{N_y} \sum_{k=1}^{N_z} \phi_{i,j,k} \psi_{i,j,k}, \quad \forall \phi, \psi \in \mathcal{C}_{\Omega},$$

and

$$[f,g]_x := \frac{1}{2}h^3 \sum_{i=1}^{N_x} \sum_{j=1}^{N_y} \sum_{k=1}^{N_z} (f_{i+\frac{1}{2},j,k}g_{i+\frac{1}{2},j,k} + f_{i-\frac{1}{2},j,k}g_{i-\frac{1}{2},j,k}), \quad \forall f,g \in \mathcal{E}_{\Omega}^x,$$

with $[\cdot,\cdot]_y$ and $[\cdot,\cdot]_z$ formulated analogously. For any $\boldsymbol{f}=(f^x,f^y,f^z)^T,\ \boldsymbol{g}=(g^x,g^y,g^z)^T\in\mathcal{E}_{\Omega}$, the discrete inner product becomes

$$(f,g) := [f^x, g^x]_x + [f^y, g^y]_y + [f^z, g^z]_z.$$

Definition 2.6. For any $f \in \mathcal{E}_{\Omega}$, we define the norm

$$\|\boldsymbol{f}\|_2 \coloneqq \sqrt{(\boldsymbol{f}, \boldsymbol{f})}.$$

In addition, for $\phi \in \mathcal{C}_{\Omega}$ we introduce the following norms:

$$\|\phi\|_{\infty} := \max_{i,j,k} |\phi_{i,j,k}|,$$

$$\|\phi\|_{p} := (|\phi|^{p}, 1)^{\frac{1}{p}}, \quad 1 \le p < \infty,$$

$$\|\nabla_{h}\phi\|_{p} := \left([|D_{x}\phi|^{p}, 1]_{x} + [|D_{y}\phi|^{p}, 1]_{y} + [|D_{z}\phi|^{p}, 1]_{z}\right)^{\frac{1}{p}}, \quad 1 \le p < \infty.$$

Observe that $(\nabla_h \phi, \nabla_h \phi) = \|\nabla_h \phi\|_2^2$, for the case p = 2.

In addition, an $(\cdot,\cdot)_{-1,h}$ inner product and $\|\cdot\|_{-1,h}$ norm need to be introduced to facilitate the analysis in later sections. For any $\varphi \in \mathring{\mathcal{C}}_{\Omega} := \{ f \in \mathcal{C}_{\Omega} \mid (f, 1) = 0 \},$ we define

$$(2.1) (\varphi_1, \varphi_2)_{-1,h} = (\varphi_1, (-\Delta_h)^{-1}\varphi_2), \|\varphi\|_{-1,h} = \sqrt{(\varphi, (-\Delta_h)^{-1}(\varphi))},$$

where the operator Δ_h is paired with discrete homogeneous Neumann boundary conditions.

We have the following Poincaré-type inequality:

Proposition 2.1. Suppose that $\Omega = (0, L)^3$, for simplicity. There is a constant C>0, independent of h>0, such that

$$\|\phi\|_2 \le C \|\nabla_h \phi\|_2,$$

for all
$$\phi \in \mathring{\mathcal{C}}_{\Omega} := \{ f \in \mathcal{C}_{\Omega} \mid (f, 1) = 0 \}.$$

2.3. Summation by parts formulas and a discrete Sobolev embedding. For $\phi, \psi \in \mathcal{C}_{\Omega}$ and a velocity vector field $\mathbf{u} \in \mathcal{E}_{\Omega}$, the following summation by parts formulas can be derived through standard calculations.

Lemma 2.1. Suppose $\phi, \psi \in \mathcal{C}_{\Omega}$ and velocity vector field $\mathbf{u} \in \mathcal{E}_{\Omega}$. If ψ satisfies the homogeneous Neumann boundary conditions $\mathbf{n} \cdot \nabla_h \phi = 0$, then

$$(\phi, \Delta_h \psi) = -(\nabla_h \phi, \nabla_h \psi).$$

If $\mathbf{u} \cdot \mathbf{n} = 0$ on the boundary, we have

$$(\phi, \nabla_h \cdot \boldsymbol{u}) = -(\nabla_h \phi, \boldsymbol{u}).$$

The following discrete Sobolev inequality has been derived in the existing works [21,22,35], for the discrete grid function with periodic boundary condition; an extension to the discrete homogeneous Neumann boundary condition can be made in a similar fashion.

Lemma 2.2 ([21,22,35]). For a grid function $f \in \mathcal{C}_{\Omega}$ satisfying the discrete homogeneous Neumann boundary condition, we have the following discrete Sobolev inequality:

(2.2)
$$||f||_4 \le C||f||_{H_h^1}, \quad \text{with } ||f||_{H_h^1}^2 := ||f||_2^2 + ||\nabla_h f||_2^2,$$

in which the positive constant C only depends on the domain Ω .

3. The fully discrete numerical scheme

For simplicity, we consider the cuboid $\Omega=(0,L)^3$ with h=L/N, for some h>0. Let $s=\frac{T}{M}>0$ be the time step size. The fully discrete scheme is proposed as follows: for $0\leq n\leq M-1$, given $\phi^n\in\mathcal{C}_\Omega$, find functions $(\phi^{n+1},\mu^{n+1},p^{n+1})\in[\mathcal{C}_\Omega]^3$, each satisfying the discrete homogeneous Neumann boundary conditions, and $\boldsymbol{u}^{n+1}\in\mathcal{E}_\Omega$, satisfying discrete no-penetration and free-slip boundary conditions, such that

(3.1)
$$\phi^{n+1} - \phi^n = s\Delta_h \mu^{n+1} - s\nabla_h \cdot (A_h \phi^n u^{n+1}),$$

(3.2)
$$\mu^{n+1} = \ln(1 + \phi^{n+1}) - \ln(1 - \phi^{n+1}) - \theta_0 \phi^n - \varepsilon^2 \Delta_h \phi^{n+1},$$

(3.3)
$$(-\Delta_h + I)\mathbf{u}^{n+1} + \nabla_h p^{n+1} + \gamma A_h \phi^n \nabla_h \mu^{n+1} = 0,$$

$$(3.4) \nabla_h \cdot \boldsymbol{u}^{n+1} = 0.$$

3.1. Positivity-preserving property and unique solvability. We begin this subsection with some preliminary definitions and results for the discrete version of the Stokes problem with no-penetration, free-slip boundary conditions.

Definition 3.1. Suppose that $\Omega=(0,L)^3$ and $\mathbf{f}\in\mathcal{E}_{\Omega}$ satisfies discrete nopenetration boundary condition on $\partial\Omega$. Let $p\in\mathring{\mathcal{C}}_{\Omega}:=\{\phi\in\mathcal{C}_{\Omega}\mid (\phi,1)=0\}$ be the unique solution to the problem

$$-\Delta_h p = \nabla_h \cdot \boldsymbol{f},$$

subject to the discrete homogeneous Neumann boundary condition $\mathbf{n} \cdot \nabla_n p = 0$. The discrete Helmholtz projection $\mathcal{P}_H^h: \{ \mathbf{f} \in \mathcal{E}_\Omega \mid \mathbf{f} \cdot \mathbf{n} = 0 \text{ on } \partial\Omega \} \to \mathcal{E}_\Omega$ is defined as follows:

$$\mathcal{P}_H^h(\boldsymbol{f}) := \boldsymbol{f} + \nabla_h p.$$

The proof of the following facts are straightforward:

Lemma 3.1. With the same assumptions as in Definition 3.1, it follows that

$$\nabla_h \cdot \mathcal{P}_H^h(\mathbf{f}) = 0.$$

Lemma 3.2. Suppose that $\Omega = (0, L)^3$ and $\mathbf{u} \in \mathcal{E}_{\Omega}$. Then

$$\nabla_h \cdot (\Delta_h \boldsymbol{u}) = \Delta_h \left(\nabla_h \cdot \boldsymbol{u} \right),$$

where the symbol Δ_h on the left is the discrete Laplacian whose domain is facecentered functions $(\mathcal{E}_{\Omega}^x, \mathcal{E}_{\Omega}^y, \text{ and } \mathcal{E}_{\Omega}^z)$ and the symbol Δ_h on the right is the discrete Laplacian whose domain is cell-centered functions (\mathcal{C}_{Ω}) .

The proof of Lemma 3.3 uses standard facts about the marker and cell (MAC) mesh points and the previous few results.

Lemma 3.3. Suppose that $\Omega = (0, L)^3$ and $\mathbf{f} \in \mathcal{E}_{\Omega}$ satisfies discrete no-penetration boundary conditions on $\partial\Omega$. Then the following two discrete problems are uniquely solvable and equivalent:

(1) Find $\mathbf{u} \in \mathcal{E}_{\Omega}$ that satisfies discrete no-penetration and discrete free-slip boundary conditions and $p \in \mathcal{C}_{\Omega}$ such that

$$-\Delta_h \boldsymbol{u} + \boldsymbol{u} + \nabla_h p = -\boldsymbol{f},$$
$$\nabla_h \cdot \boldsymbol{u} = 0.$$

(2) Find $\mathbf{u} \in \mathcal{E}_{\Omega}$ that satisfies discrete no-penetration and discrete free-slip boundary conditions such that

$$-\Delta_h \boldsymbol{u} + \boldsymbol{u} = -\mathcal{P}_H^h(\boldsymbol{f}).$$

Lemma 3.4. For any $\phi^n \in \mathcal{C}_{\Omega}$, define a linear operator $\mathcal{L}_h : \mathring{\mathcal{C}}_{\Omega} \to \mathring{\mathcal{C}}_{\Omega} := \{ \phi \in \mathcal{C}_{\Omega} \mid (\phi, 1) = 0 \}$ via

(3.5)
$$\mathcal{L}_h(\mu) = s\nabla_h \cdot (A_h \phi^n \mathbf{u}_\mu) - s\Delta_h \mu,$$

where $\mathbf{u}_{\mu} \in \mathcal{E}_{\Omega}$ is the unique vector grid function that satisfies discrete no-penetration and free-slip boundary conditions and the equation

(3.6)
$$S_h \mathbf{u}_{\mu} = -\gamma \mathcal{P}_H^h (A_h \phi^n \nabla_h \mu),$$

where $S_h := -\Delta_h + I$. Then the following conclusions are valid: (i) For any $\phi \in \mathring{\mathcal{C}}_{\Omega}$, there is a unique $\mu \in \mathring{\mathcal{C}}_{\Omega}$ that satisfies $\mathcal{L}_h(\mu) = \phi$, and (ii) for any $\mu \in \mathring{\mathcal{C}}_{\Omega}$, we have $\|\mathcal{L}_h^{-1}(\mu)\|_{\infty} \leq Cs^{-1}h^{-3/2}\|\mu\|_{\infty}$.

Proof. Clearly \mathcal{L}_h is linear. Given $\mu_1, \mu_2 \in \mathring{\mathcal{C}}_{\Omega}$, a careful calculation reveals that

$$(\mu_{1}, \mathcal{L}_{h}(\mu_{2})) = (\mu_{1}, s\nabla_{h} \cdot (A_{h}\phi^{n}\boldsymbol{u}_{\mu_{2}}) - s\Delta_{h}\mu_{2})$$

$$= s(\nabla_{h}\mu_{1}, \nabla_{h}\mu_{2}) - s(A_{h}\phi^{n}\nabla_{h}\mu_{1}, \boldsymbol{u}_{\mu_{2}})$$

$$= s(\nabla_{h}\mu_{1}, \nabla_{h}\mu_{2}) + \frac{s}{\gamma}(S_{h}\boldsymbol{u}_{\mu_{1}}, \boldsymbol{u}_{\mu_{2}})$$

$$= s(\nabla_{h}\mu_{1}, \nabla_{h}\mu_{2}) + \frac{s}{\gamma}(\boldsymbol{u}_{\mu_{1}}, \boldsymbol{u}_{\mu_{2}}) + \frac{s}{\gamma}(\nabla_{h}\boldsymbol{u}_{\mu_{1}}, \nabla_{h}\boldsymbol{u}_{\mu_{2}}),$$

$$= s(\nabla_{h}\mu_{1}, \nabla_{h}\mu_{2}) + \frac{s}{\gamma}(\boldsymbol{u}_{\mu_{1}}, \boldsymbol{u}_{\mu_{2}}) + \frac{s}{\gamma}(\nabla_{h}\boldsymbol{u}_{\mu_{1}}, \nabla_{h}\boldsymbol{u}_{\mu_{2}}),$$

where summation by parts formulas have been repeatedly applied. We conclude that the operator is symmetric:

$$(\mu_1, \mathcal{L}_h(\mu_2)) = (\mathcal{L}_h(\mu_1), \mu_2).$$

The expansion (3.7) implies that

$$(3.8) \qquad (\mu, \mathcal{L}_h(\mu)) = s \|\nabla_h \mu\|_2^2 + \frac{s}{\gamma} \|\boldsymbol{u}_{\mu}\|_2^2 + \frac{s}{\gamma} \|\nabla_h \boldsymbol{u}_{\mu}\|_2^2 \ge s \|\nabla_h \mu\|_2^2 \ge s C_1^2 \|\mu\|_2^2,$$

where C_1 is the constant associated with the discrete Poincaré inequality. Thus \mathcal{L}_h is SPD on the space $\mathring{\mathcal{C}}_{\Omega}$ and is, therefore, invertible.

Furthermore, equation (3.8) reveals that

$$\lambda_{min}(\mathcal{L}_h) \ge sC_1^2$$
 and $\lambda_{max}(\mathcal{L}_h^{-1}) \le \frac{1}{sC_1^2}$,

where λ_{min} , λ_{max} refer to the smallest and largest positive eigenvalues of a symmetric, positive definite operator. Then we get

$$\|\mathcal{L}_h^{-1}(\mu)\|_2 \le \frac{1}{sC_1^2} \|\mu\|_2,$$

for any $\mu \in \mathring{\mathcal{C}}_{\Omega}$. By the 3-D inverse inequality, the following result is obtained:

$$\|\mathcal{L}_{h}^{-1}(\mu)\|_{\infty} \leq \frac{C_{2} \|\mathcal{L}_{h}^{-1}(\mu)\|_{2}}{h^{3/2}} \leq C_{2} s^{-1} C_{1}^{-2} h^{-3/2} \|\mu\|_{2}$$
$$\leq C_{2} s^{-1} C_{1}^{-2} |\Omega|^{\frac{1}{2}} h^{-3/2} \|\mu\|_{\infty},$$

where the last step comes from an obvious fact, $||f||_2 \le |\Omega|^{\frac{1}{2}} ||f||_{\infty}$. The proof is complete.

The positivity-preserving and unique solvability properties are established in Theorem 3.1.

Theorem 3.1. Assume that $\phi^n \in \mathcal{C}_{\Omega}$ is given, with $\|\phi^n\|_{\infty} \leq M$ and $-1 < \overline{\phi^n} =: \beta < 1$. There exists a unique solution $\phi^{n+1} \in \mathcal{C}_{\Omega}$ to (3.1)–(3.4), with $(\phi^{n+1} - \phi_0, 1) = 0$ and $\|\phi^{n+1}\|_{\infty} < 1$.

Proof. For any
$$\phi \in A_h := \{ \phi \in \mathcal{C}_{\Omega} \mid \|\phi\|_{\infty} \le 1, \ (\phi - \beta, 1) = 0 \}$$
, define
$$\mathcal{J}(\phi) := (\mathcal{L}_h^{-1}(\phi - \phi^n), \phi - \phi^n) + (1 + \phi, \ln(1 + \phi)) + (1 - \phi, \ln(1 - \phi))$$
$$+ \frac{\varepsilon^2}{2} \|\nabla_h \phi\|_2^2 - \theta_0(\phi, \phi^n).$$

The solution of the numerical scheme is a minimizer of this discrete functional. Subsequently, we define

$$\mathcal{F}(\psi) := \mathcal{J}(\psi + \beta), \quad \forall \, \psi \in \mathring{A}_h := \left\{ \psi \in \mathcal{C}_{\Omega} \mid (\phi, 1) = 0, \ -1 - \beta \le \psi \le 1 - \beta \right\}.$$

It is clear that, if $\psi \in \mathring{A}_h$ minimizes \mathcal{F} , then $\psi + \beta \in A_h$ minimizes \mathcal{J} .

Next, let us define the following closed domain:

$$\mathring{A}_{h,\delta} := \{ \psi \in \mathcal{C}_{\Omega} \mid (\psi, 1) = 0, -1 - \beta + \delta \le \psi \le 1 - \beta - \delta \},$$

where $\delta \in (0, 1/2)$ and is sufficiently small. Since $\mathring{A}_{h,\delta}$ is a bounded, compact and convex set in \mathring{C}_{Ω} , there exists a (not necessarily unique) minimizer of \mathcal{F} over $\mathring{A}_{h,\delta}$. The key point of the positivity analysis is that such a minimizer could not occur on the boundary of $\mathring{A}_{h,\delta}$, if δ is sufficiently small. To be more explicit, by the boundary of $\mathring{A}_{h,\delta}$, we mean the locus of points $\psi \in \mathring{A}_{h,\delta}$ such that $\|\psi + \beta\|_{\infty} = 1 - \delta$.

To get a contradiction, suppose that the minimizer of \mathcal{F} , call it ϕ^* , occurs at a boundary point of $\mathring{A}_{h,\delta}$. There is at least one grid point $\vec{\alpha}_0 = (i_0, j_0, k_0)$ such that $|\phi^*_{\vec{\alpha}_0} + \beta| = 1 - \delta$. First, we assume that $\phi^*_{\vec{\alpha}_0} + \beta = \delta - 1$, so that the grid

function ϕ^* has a global minimum at $\vec{\alpha}_0$. Suppose that ϕ^* achieves its maximum at $\vec{\alpha}_1 = (i_1, j_1, k_1)$. By the fact that $\bar{\phi}^* = 0$, we have $\phi^*_{\vec{\alpha}_1} \geq 0$ and then

$$(3.9) 1 - \delta \ge \varphi_{\vec{\alpha}_1}^{\star} + \beta \ge \beta.$$

Since \mathcal{F} is smooth over $\mathring{A}_{h,\delta}$, for all $\psi \in \mathring{\mathcal{C}}_{\Omega}$, the directional derivative turns out to be

(3.10)

$$d_s \mathcal{F}(\phi^* + s\psi)|_{s=0} = (\ln(1 + \phi^* + \beta) - \ln(1 - \phi^* - \beta), \psi) - (\theta_0 \phi^n + \varepsilon^2 \Delta_h \phi^*, \psi) + (\mathcal{L}_h^{-1}(\phi^* - \phi^n + \beta), \psi).$$

Pick the direction ψ as

$$\psi_{i,j,k} = \delta_{i,i_0} \delta_{j,j_0} \delta_{k,k_0} - \delta_{i,i_1} \delta_{j,j_1} \delta_{k,k_1}.$$

Then the derivative can be expressed as

(3.11)

$$\frac{1}{h^{3}}d_{s}\mathcal{F}(\phi^{*}+s\psi)|_{s=0} = \ln(1+\phi_{\vec{\alpha}_{0}}^{*}+\beta) - \ln(1-\phi_{\vec{\alpha}_{0}}^{*}-\beta) - \ln(1+\phi_{\vec{\alpha}_{1}}^{*}+\beta)
+ \ln(1-\phi_{\vec{\alpha}_{1}}^{*}-\beta)
- \theta_{0}(\phi_{\vec{\alpha}_{0}}^{n}-\phi_{\vec{\alpha}_{1}}^{n}) - \varepsilon^{2}(\Delta_{h}\phi_{\vec{\alpha}_{0}}^{*}-\Delta\phi_{\vec{\alpha}_{1}}^{*})
+ \mathcal{L}_{h}^{-1}(\phi^{*}-\phi^{n}+\beta)_{\vec{\alpha}_{0}} - \mathcal{L}_{h}^{-1}(\phi^{*}-\phi^{n}+\beta)_{\vec{\alpha}_{1}}.$$

By the fact that $\beta + \phi_{\vec{\alpha}_0}^* = -1 + \delta$ and (3.9), we have (3.12)

$$\ln(1+\phi_{\vec{\alpha}_0}^*+\beta) - \ln(1-\phi_{\vec{\alpha}_0}^*-\beta) - \ln(1+\phi_{\vec{\alpha}_1}^*+\beta) + \ln(1-\phi_{\vec{\alpha}_1}^*-\beta) \le \ln\frac{\delta}{2-\delta} - \ln\frac{1+\beta}{1-\beta}.$$

Since ϕ^* takes a minimum at the grid point $\vec{\alpha}_0$ and a maximum at the grid point $\vec{\alpha}_1$, it is obvious that

$$(3.13) \Delta_h \phi_{\vec{\alpha}_0}^* \ge 0, \Delta_h \phi_{\vec{\alpha}_1}^* \le 0, \Longrightarrow -\varepsilon^2 (\Delta_h \phi_{\vec{\alpha}_0}^* - \Delta \phi_{\vec{\alpha}_1}^*) \le 0.$$

By the assumption that $\|\phi^n\| \leq M$, the following inequality is straightforward:

$$(3.14) -2M \le \phi_{\vec{\alpha}_0}^n - \phi_{\vec{\alpha}_1}^n \le 2M.$$

Setting $\mu^* = \mathcal{L}_h^{-1}(\phi^* - \phi^n + \beta)$, we obtain

$$\|\mathcal{L}_{h}(\mu^{*})\|_{\infty} = s\|\nabla_{h} \cdot ((1 + \gamma(A_{h}\phi^{n})^{2})\nabla_{h}\mu^{*}) + \nabla_{h} \cdot (A_{h}\phi^{n}\nabla_{h}p_{\mu^{*}})\|_{\infty}$$

$$= \|\phi^{*} - \phi^{n} + \beta\|_{\infty}$$

$$< M + 1.$$

Therefore, an application of Lemma 3.4 implies that (3.16)

$$\|\mathcal{L}_h^{-1}(\phi^* - \phi^n + \beta)\|_{\infty} = \|\mu^*\|_{\infty} \le Cs^{-1}h^{-3/2}\|\mathcal{L}_h(\mu^*)\|_{\infty} \le Cs^{-1}h^{-3/2}(M+1).$$

A combination of (3.11) to (3.16) leads to

$$(3.17) \frac{1}{h^3} d_s \mathcal{F}(\phi^* + s\psi)|_{s=0} \le \ln \frac{\delta}{2 - \delta} - \ln \frac{1 + \beta}{1 - \beta} + 2\theta_0 M + 2Cs^{-1}h^{-3/2}(M + 1).$$

Notice that right hand side of (3.17) is singular as $s, h \to 0$. Meanwhile, for any fixed s, h > 0, we may choose $\delta \in (0, 1/2)$ sufficiently small so that

(3.18)
$$d_s \mathcal{F}(\phi^* + s\psi)|_{s=0} < 0.$$

This contradicts the assumption that \mathcal{F} has a minimum at ϕ^* , since the directional derivative is negative in a direction pointing into the interior of $\mathring{A}_{h.\delta}$.

Using similar arguments, we can also prove that the global minimum of \mathcal{F} over $\mathring{A}_{h,\delta}$ could not occur at a boundary point ϕ^* such that $\phi^*_{\vec{\alpha}_0} + \beta = 1 - \delta$. The details are left to interested readers.

A combination of these two facts reveals that the global minimum of \mathcal{F} over $\mathring{A}_{h,\delta}$ could only possibly occur at interior point if δ sufficiently small. Therefore, there must be a solution $\phi + \beta \in A_h$ that minimizes \mathcal{J} over A_h , which is equivalent to the numerical solution of (3.1)–(3.4). The existence of the numerical solution is established.

Finally, since \mathcal{J} is a strictly convex function over A_h , the uniqueness analysis of numerical solution is straightforward.

3.2. Unconditional energy stability. Now we establish an unconditional energy stability of the proposed numerical scheme. For any $\phi \in \mathcal{C}_{\Omega}$, its discrete energy is defined as

$$F_h(\phi) = \left((1+\phi)\ln(1+\phi) + (1-\phi)\ln(1-\phi) - \frac{\theta_0}{2}\phi^2, 1 \right) + \frac{\varepsilon^2}{2} \|\nabla_h \phi\|_2^2.$$

The following discrete energy dissipation result is valid.

Theorem 3.2. Numerical solutions of (3.1)—(3.4) are unconditionally energy stable in the sense that

(3.19)
$$F_h(\phi^{n+1}) - F_h(\phi^n) \le -\frac{\varepsilon^2}{2} \|\nabla_h(\phi^{n+1} - \phi^n)\|_2^2 - s\|\nabla_h\mu^{n+1}\|_2^2 - \frac{s}{\gamma} (\|\boldsymbol{u}^{n+1}\|_2^2 + \|\nabla_h\boldsymbol{u}^{n+1}\|_2^2).$$

Proof. The following definitions are introduced for simplicity of presentation:

$$G(\phi) := F_1(\phi) - F_2(\phi),$$

(3.20)
$$F_1(\phi) := (1+\phi)\ln(1+\phi) + (1-\phi)\ln(1-\phi), \quad F_2(\phi) := \frac{\theta_0}{2}\phi^2,$$
$$f_1(\phi) := F_1'(\phi) = \ln(1+\phi) - \ln(1-\phi), \quad f_2(\phi) := F_2'(\phi) = \theta_0\phi.$$

Taking an inner production with (3.1) by the chemical potential μ^{n+1} gives

(3.21)
$$\frac{1}{s}(\phi^{n+1} - \phi^n, \mu^{n+1}) = (\Delta_h \mu^{n+1}, \mu^{n+1}) - (\nabla_h \cdot (A_h \phi^n \boldsymbol{u}^{n+1}), \mu^{n+1})$$
$$= -\|\nabla_h \mu^{n+1}\|_2^2 - (\nabla_h \cdot (A_h \phi^n \boldsymbol{u}^{n+1}), \mu^{n+1}).$$

Meanwhile, taking an inner production with (3.2) by $\phi^{n+1} - \phi^n$ yields

$$(\phi^{n+1} - \phi^{n}, \mu^{n+1})$$

$$= (f_{1}(\phi^{n+1}) - f_{2}(\phi^{n}), \phi^{n+1} - \phi^{n}) - (\varepsilon^{2}\Delta_{h}\phi^{n+1}, \phi^{n+1} - \phi^{n})$$

$$= (f_{1}(\phi^{n+1}) - f_{2}(\phi^{n}), \phi^{n+1} - \phi^{n}) + \varepsilon^{2}(\nabla_{h}\phi^{n+1}, \nabla_{h}(\phi^{n+1} - \phi^{n}))$$

$$= (f_{1}(\phi^{n+1}) - f_{2}(\phi^{n}), \phi^{n+1} - \phi^{n}) + \frac{\varepsilon^{2}}{2}(\|\nabla_{h}(\phi^{n+1} - \phi^{n})\|_{2}^{2}$$

$$+ \|\nabla_{h}\phi^{n+1}\|_{2}^{2} - \|\nabla_{h}\phi^{n}\|_{2}^{2}).$$

A combination of (3.21) and (3.22) results in (3.23)

$$(f_1(\phi^{n+1}) - f_2(\phi^n), \phi^{n+1} - \phi^n) + \frac{\varepsilon^2}{2} (\|\nabla_h(\phi^{n+1} - \phi^n)\|_2^2 + \|\nabla_h\phi^{n+1}\|_2^2 - \|\nabla_h\phi^n\|_2^2) + s\|\nabla_h\mu^{n+1}\|_2^2 - s(A_h\phi^n\boldsymbol{u}^{n+1}, \nabla_h\mu^{n+1}) = 0.$$

On the other hand, the convexity of F_1 and F_2 reveals the following inequalities:

$$(3.24) F_1(\phi^{n+1}) - F_1(\phi^n) \le f_1(\phi^{n+1})(\phi^{n+1} - \phi^n),$$

(3.25)
$$F_2(\phi^{n+1}) - F_2(\phi^n) \ge f_2(\phi^n) \left(\phi^{n+1} - \phi^n\right),$$

which in turn lead to

$$(3.26) (G(\phi^{n+1}) - G(\phi^n), 1) \le (f_1(\phi^{n+1}) - f_2(\phi^n), \phi^{n+1} - \phi^n).$$

As a result, a combination of (3.21) and (3.26) implies that

$$(G(\phi^{n+1}) - G(\phi^{n}), 1) + \frac{\varepsilon^{2}}{2} (\|\nabla_{h}(\phi^{n+1} - \phi^{n})\|_{2}^{2} + \|\nabla_{h}\phi^{n+1}\|_{2}^{2} - \|\nabla_{h}\phi^{n}\|_{2}^{2})$$

$$+ s\|\nabla_{h}\mu^{n+1}\|_{2}^{2} - s(A_{h}\phi^{n}\boldsymbol{u}^{n+1}, \nabla_{h}\mu^{n+1})$$

$$\leq 0.$$

Finally, the following estimate could be derived: (3.28)

$$F_{h}(\phi^{n+1}) - F_{h}(\phi^{n})$$

$$\leq -\frac{\varepsilon^{2}}{2} \|\nabla_{h}(\phi^{n+1} - \phi^{n})\|_{2}^{2} - s\|\nabla_{h}\mu^{n+1}\|_{2}^{2} + s(\boldsymbol{u}^{n+1}, A_{h}\phi^{n}\nabla_{h}\mu^{n+1})$$

$$= -\frac{\varepsilon^{2}}{2} \|\nabla_{h}(\phi^{n+1} - \phi^{n})\|_{2}^{2} - s\|\nabla_{h}\mu^{n+1}\|_{2}^{2} - \frac{s}{\gamma}(\boldsymbol{u}^{n+1}, \mathcal{S}_{h}\boldsymbol{u}^{n+1} + \nabla_{h}p^{n+1})$$

$$= -\frac{\varepsilon^{2}}{2} \|\nabla_{h}(\phi^{n+1} - \phi^{n})\|_{2}^{2} - s\|\nabla_{h}\mu^{n+1}\|_{2}^{2} - \frac{s}{\gamma}(\|\boldsymbol{u}^{n+1}\|_{2}^{2} + \|\nabla_{h}\boldsymbol{u}^{n+1}\|_{2}^{2}),$$

where summation by parts formulas have been repeatedly applied. This finishes the proof. $\hfill\Box$

4. Convergence analysis

Now we proceed into the convergence analysis. Let (Φ, U, P) be the exact PDE solution for the CHS system (1.1)–(1.4). With sufficiently regular initial data, it is reasonable to assume that the exact solution has regularity of class \mathcal{R} , where

(4.1)
$$\Phi \in \mathcal{R} := H^4(0, T; C(\Omega)) \cap H^3(0, T; C^2(\Omega)) \cap L^{\infty}(0, T; C^6(\Omega)).$$

In addition, we assume that the following separation property is valid for the exact solution:

(4.2)
$$1 + \Phi \ge \epsilon_0$$
, $1 - \Phi \ge \epsilon_0$, for some $\epsilon_0 > 0$, at a point-wise level.

Define $\Phi_N(\cdot,t) = \mathcal{P}_N\Phi(\cdot,t)$, $U_N(\cdot,t) = \mathcal{P}_NU(\cdot,t)$, $P_N(\cdot,t) = \mathcal{P}_NP(\cdot,t)$, the spatial Fourier projection of the exact solution into \mathcal{B}^K , the space of trigonometric polynomials of degree to and including K with N = 2K + 1. The following projection approximation is standard: if $(\Phi, U, P) \in L^{\infty}(0, T; H^{\ell}_{per}(\Omega))$, for any $\ell \in \mathbb{N}$

with $0 \le k \le \ell$,

(4.3)
$$\|\Phi_{N} - \Phi\|_{L^{\infty}(0,T;H^{k})} \leq Ch^{\ell-k} \|\Phi\|_{L^{\infty}(0,T;H^{\ell})},$$

$$\|U_{N} - U\|_{L^{\infty}(0,T;H^{k})} \leq Ch^{\ell-k} \|U\|_{L^{\infty}(0,T;H^{\ell})},$$

$$\|P_{N} - P\|_{L^{\infty}(0,T;H^{k})} \leq Ch^{\ell-k} \|P\|_{L^{\infty}(0,T;H^{\ell})}.$$

In fact, the Fourier projection estimate does not automatically preserve the positivity of $1 + \Phi_N$ and $1 - \Phi_N$; on the other hand, we could enforce the phase separation property that $1 + \Phi_N \ge \frac{1}{2}\epsilon_0$, $1 - \Phi_N \ge \frac{1}{2}\epsilon_0$, if h is taken sufficiently small.

property that $1 + \Phi_N \ge \frac{1}{2}\epsilon_0$, $1 - \Phi_N \ge \frac{1}{2}\epsilon_0$, if h is taken sufficiently small. We denote $\Phi_N(\cdot, t_n)$ by Φ_N^n . Since $\Phi_N^n \in \mathcal{B}^K$, the mass conservative property is available at the discrete level:

(4.4)
$$\overline{\Phi_N^n} = \frac{1}{|\Omega|} \int_{\Omega} \Phi_N(\cdot, t_n) d\mathbf{x} = \frac{1}{|\Omega|} \int_{\Omega} \Phi_N(\cdot, t_{n-1}) d\mathbf{x} = \overline{\Phi_N^{n-1}},$$

for any $n \in \mathbb{N}$. On the other hand, the numerical solution (3.1) is also mass conservative at the discrete level:

(4.5)
$$\overline{\phi^n} = \overline{\phi^{n-1}}, \ \overline{\phi^n} = \overline{\phi^{n-1}}, \ \forall \ n \in \mathbb{N}.$$

In turn, the error grid function is defined as

$$(4.6) e_{\phi}^{n} := \mathcal{P}_{N} \Phi_{N}^{n} - \phi^{n}, e_{\mathbf{v}}^{n} := \mathcal{P}_{N} \mathbf{U}_{N}^{n} - \mathbf{u}^{n}, e_{p}^{n} := \mathcal{P}_{N} P_{N}^{n} - p^{n}, \forall n \in \mathbb{N}.$$

It follows that $\overline{e_{\phi}^n} = 0$, for any $n \in N$, so that the discrete norm $\|\cdot\|_{-1,h}$ is well defined for the error grid function e_{ϕ}^n .

Theorem 4.1 is the main result of this section.

Theorem 4.1. Given initial data $\Phi(\cdot, t = 0) \in C^6(\Omega)$, suppose the exact solution for CHS equations (1.1)—(1.4) is of regularity class \mathcal{R} . Provided that s and h are sufficiently small and under a requirement $C_1h \leq s \leq C_2h$, we have

(4.7)
$$\|\nabla_h e_{\phi}^n\|_2 + \left(s \sum_{k=1}^n \|\nabla_h \Delta_h e_{\phi}^k\|_2^2\right)^{\frac{1}{2}} \le C(s+h^2),$$

for all positive integers n, such that $t_n = n \cdot s < T$, where C > 0 is independent of s, h and n.

4.1. Higher order truncation error estimate. By consistency, the projection solution (Φ_N, U_N, P_N) solves the discrete equations (3.1)–(3.4) with a first order accuracy in time and second order accuracy in space. Meanwhile, it is observed that this leading local truncation error will not be sufficient to obtain an ℓ^{∞} bound for the numerical solution to recover the separation property, as well as a $W_h^{1,4}$ bound to pass through the convergence estimate. To overcome this difficulty, we build a higher order consistency analysis via a perturbation term. In more details, we need to construct supplementary fields $\Phi_{\Delta t}$, $U_{\Delta t}$, $P_{\Delta t}$ and define the following profiles

$$(4.8) \qquad \hat{\Phi} = \Phi_N + s\mathcal{P}_N \Phi_{\Delta t}, \quad \hat{U} = \mathcal{P}\mathcal{H}_h(U_N + s\mathcal{P}_N U_{\Delta t}), \quad \hat{P} = P_N + s\mathcal{P}_N P_{\Delta t},$$

in which a special interpolation operator \mathcal{PH}_h , which will be introduced later, enforces the divergence-free condition at a discrete level.

The following truncation error analysis for the temporal discretization can be obtained by using a straightforward Taylor expansion as well as estimate (4.3) for

the projection solution:

(4.9)
$$\frac{\Phi_N^{n+1} - \Phi_N^n}{s} = \Delta \mathcal{V}_N^{n+1} - \nabla \cdot (\Phi_N^n U_N^{n+1}) + s(G_\phi^{(0)})^n + O(s^2) + O(h^{m_0}),$$

$$(4.10) \quad \mathcal{V}_N^{n+1} = \ln(1 + \Phi_N^{n+1}) - \ln(1 - \Phi_N^{n+1}) - \theta_0 \Phi_N^n - \varepsilon^2 \Delta \Phi_N^{n+1},$$

$$(4.11) \quad (-\Delta + I)\boldsymbol{U}_{N}^{n+1} = -\nabla P_{N}^{n+1} - \gamma \Phi_{N}^{n} \nabla \mathcal{V}_{N}^{n+1} + s(G_{v}^{(0)})^{n} + O(s^{2}) + O(h^{m_{0}}),$$

$$(4.12) \quad \nabla \cdot \boldsymbol{U}_{N}^{n+1} = 0,$$

with the homogeneous Neumann boundary condition for Φ_N , no-penetration, free slip boundary condition for U_N , in a similar form as in (1.5). Here $m_0 \geq 4$ and $G_{\phi}^{(0)}$, $G_v^{(0)}$ can be assumed to be smooth enough in the sense that their derivatives are bounded.

The correction function $(\Phi_{\Delta t}, \boldsymbol{U}_{\Delta t}, P_{\Delta t})$ is given by solving the following equation:

$$(4.13) \ \partial_t \Phi_{\Delta t} = -\nabla \cdot (\Phi_N \boldsymbol{U}_{\Delta t} + \Phi_{\Delta t} \boldsymbol{U}_N) + \Delta \mathcal{V}_{\Delta t} - G_{\phi}^{(0)},$$

$$(4.14) \ \mathcal{V}_{\Delta t} = \frac{\Phi_{\Delta t}}{1 + \Phi_{N}} + \frac{\Phi_{\Delta t}}{1 - \Phi_{N}} - \theta_0 \Phi_{\Delta t} - \varepsilon^2 \Delta \Phi_{\Delta t},$$

$$(4.15) (-\Delta + I)\boldsymbol{U}_{\Delta t} = -\nabla P_{\Delta t} - \gamma(\Phi_N \nabla \mathcal{V}_{\Delta t} + \Phi_{\Delta t} \nabla \mathcal{V}_N) - G_v^{(0)}, \quad \nabla \cdot \boldsymbol{U}_{\Delta t} = 0,$$

with the homogeneous Neumann boundary condition for $\Phi_{\Delta t}$, no-penetration, free slip boundary condition for $U_{\Delta t}$. Existence of a solution of the above linear, convection-diffusion type PDE is straightforward. Since the correction function depends only on the projection solution (Φ_N, U_N, P_N) with enough regularity, the derivatives of $(\Phi_{\Delta t}, U_{\Delta t}, P_{\Delta t})$ in various orders are bounded. Subsequently, an application of the semi-implicit discretization implies that

$$\frac{\Phi_{\Delta t}^{n+1} - \Phi_{\Delta t}^{n}}{s} = -\nabla \cdot (\Phi_{N}^{n} \boldsymbol{U}_{\Delta t}^{n+1} + \Phi_{\Delta t}^{n} \boldsymbol{U}_{N}^{n+1}) + \Delta \mathcal{V}_{\Delta t}^{n+1} - (G_{\phi}^{(0)})^{n} + O(s),$$

(4.17)

$$\mathcal{V}_{\Delta t}^{n+1} = \frac{\Phi_{\Delta t}^{n+1}}{1 + \Phi_{N}^{n+1}} + \frac{\Phi_{\Delta t}^{n+1}}{1 - \Phi_{N}^{n+1}} - \theta_0 \Phi_{\Delta t}^n - \varepsilon^2 \Delta \Phi_{\Delta t}^{n+1},$$

(4.18)

$$(-\Delta + I)\boldsymbol{U}_{\Delta t}^{n+1} = -\nabla P_{\Delta t}^{n+1} - \gamma(\Phi_N^n \nabla \mathcal{V}_{\Delta t}^{n+1} + \Phi_{\Delta t}^n \nabla \mathcal{V}_N^{n+1}) - (G_v^{(0)})^n + O(s),$$

(4.19)

$$\nabla \cdot \boldsymbol{U}_{\Delta t}^{n+1} = 0.$$

Therefore, a combination of (4.9)–(4.12) and (4.16)–(4.19) leads to a second order temporal truncation error of $\hat{\Phi}_1 = \Phi_N + s\mathcal{P}_N\Phi_{\Delta t}$, $\hat{U}_1 = U_N + s\mathcal{P}_NU_{\Delta t}$, $\hat{P}_1 = P_N + s\mathcal{P}_NP_{\Delta t}$:

$$(4.20) \qquad \frac{\hat{\Phi}_1^{n+1} - \hat{\Phi}_1^n}{s} = -\nabla \cdot (\hat{\Phi}_1^n \hat{\boldsymbol{U}}_1^{n+1}) + \Delta \hat{\mathcal{V}}_1^{n+1} + O(s^2),$$

$$(4.21) \qquad \hat{\mathcal{V}}_1^{n+1} = \ln(1 + \hat{\Phi}_1^{n+1}) - \ln(1 - \hat{\Phi}_1^{n+1}) - \theta_0 \hat{\Phi}_1^n - \varepsilon^2 \Delta \hat{\Phi}_1^{n+1},$$

$$(4.22) \qquad (-\Delta + I)\hat{\boldsymbol{U}}_{1}^{n+1} = -\nabla \hat{P}_{1}^{n+1} - \gamma(\hat{\Phi}_{1}^{n}\nabla\hat{\mathcal{V}}_{1}^{n+1}) + O(s^{2}), \quad \nabla \cdot \hat{\boldsymbol{U}}_{1}^{n+1} = 0.$$

The homogeneous Neumann boundary condition is satisfied for $\hat{\Phi}_1$, while a nopenetration, free slip boundary condition is satisfied for \hat{U}_1 . In the derivation of

(4.20) – (4.22), the following linearized expansions have been utilized:

(4.23)
$$\ln(1 \pm \hat{\Phi}_1) = \ln(1 \pm \Phi_N \pm s\hat{\Phi}_{\Delta t}) = \ln(1 \pm \Phi_N) + \frac{\hat{\Phi}_{\Delta t}s}{1 + \Phi_N} + O(s^2),$$

$$(4.24) \qquad \hat{\Phi}_1^n \hat{\boldsymbol{U}}_1^{n+1} = \Phi_N^n \boldsymbol{U}_N^{n+1} + s(\Phi_{\Delta t}^n \boldsymbol{U}_N^{n+1} + \Phi_N^n \boldsymbol{U}_{\Delta t}^{n+1}) + O(s^2),$$

$$(4.25) \qquad \hat{\Phi}_1^n \nabla \widehat{\mathcal{V}}_1^{n+1} = \Phi_N^n \nabla \mathcal{V}_N^{n+1} + s(\Phi_{\Delta t}^n \nabla \mathcal{V}_N^{n+1} + \Phi_N^n \nabla \mathcal{V}_{\Delta t}^{n+1}) + O(s^2).$$

In terms of the spatial discretization, the velocity profile $\hat{\boldsymbol{U}}_1$ is not divergencefree at a discrete level, so that its discrete inner product with the pressure gradient may not vanish. To overcome the difficulty, we propose a spatial interpolation operator \mathcal{PH}_h defined as follows, for any $\boldsymbol{u} \in H^1(\Omega)$, $\nabla \cdot \boldsymbol{u} = 0$:

There is an exact stream function vector $\boldsymbol{\psi} = (\psi_1, \ \psi_2, \ \psi_3)^T$ so that $\boldsymbol{u} = \nabla^{\perp} \boldsymbol{\psi}$,

$$(4.26) \mathcal{P}\mathcal{H}_h(\mathbf{u}) = \nabla_h^{\perp} \psi = (D_y \psi_3 - D_z \psi_2, D_z \psi_1 - D_x \psi_3, D_x \psi_2 - D_y \psi_1)^T.$$

This definition guarantees $\nabla_h \cdot \mathcal{PH}_h(\boldsymbol{u}) = 0$ at a point-wise level. Consequently, we obtain the definition of (4.8) and the higher order truncation error for $(\hat{\boldsymbol{\Phi}}, \hat{\boldsymbol{U}}, \hat{\boldsymbol{P}})$:

(4.27)
$$\frac{\hat{\Phi}^{n+1} - \hat{\Phi}^n}{s} = -\nabla_h \cdot (A_h \hat{\Phi}^n \hat{U}^{n+1}) + \Delta_h \hat{\mathcal{V}}^{n+1} + \tau_\phi^{n+1},$$

$$(4.28) \qquad \hat{\mathcal{V}}^{n+1} = \ln(1 + \hat{\Phi}^{n+1}) - \ln(1 - \hat{\Phi}^{n+1}) - \theta_0 \hat{\Phi}^n - \varepsilon^2 \Delta_h \hat{\Phi}^{n+1},$$

$$(4.29) \qquad (-\Delta_h + I)\hat{\boldsymbol{U}}^{n+1} = -\nabla_h \hat{P}^{n+1} - \gamma (A_h \phi^n \nabla_h \hat{\mathcal{V}}^{n+1}) + \tau_v^{n+1},$$

$$(4.30) \qquad \nabla_h \cdot \hat{\boldsymbol{U}}^{n+1} = 0,$$

where

(4.31)
$$\|\tau_{\phi}^{n+1}\|_{2}, \ \|\tau_{v}^{n+1}\|_{2} \leq O(s^{2} + h^{2}).$$

In addition, a discrete homogeneous Neumann boundary condition is for $\hat{\Phi}$, and a discrete no-penetration, free slip boundary condition for \hat{U} is satisfied.

The reason for such a higher truncation error estimate is to derive an ℓ^{∞} bound for the numerical solution, which is needed to obtain the separation property in the rough error estimate. With such a property for the constructed approximate solution and the numerical solution, the nonlinear error term could be appropriately analyzed in the $\ell^{\infty}(0,T;H_h^1)$ convergence estimate.

Remark 4.1. Trivial initial data $\Phi_{\Delta t}(\cdot, t=0) \equiv 0$ are imposed, as in (4.16)–(4.18). Therefore using similar process in (4.4)–(4.5), we have

(4.32)
$$\phi^0 \equiv \hat{\Phi}^0, \quad \overline{\phi^k} = \overline{\phi^0}, \quad \forall k \ge 0,$$

(4.33)
$$\overline{\hat{\Phi}^k} = \frac{1}{|\Omega|} \int_{\Omega} \hat{\Phi}(\cdot, t_k) \, d\mathbf{x} = \frac{1}{|\Omega|} \int_{\Omega} \hat{\Phi}^0 \, d\mathbf{x} = \overline{\phi^0}, \quad \forall \, k \ge 0,$$

where the first step is based on the fact that $\hat{\Phi} \in \mathcal{B}^K$, and the second step comes from the mass conservative property of $\hat{\Phi}$ at the continuous level. These two properties will be used in the later analysis.

In addition, since $\hat{\Phi}$ is mass conservative at a discrete level, we observe that the local truncation error τ_{ϕ} has a similar property:

$$(4.34) \overline{\tau_{\phi}^{n+1}} = 0, \quad \forall n \ge 0.$$

Remark 4.2. Since the correction function $\Phi_{\Delta t}$ is bounded, we recall the separation property (4.2) for the exact solution, and obtain a similar property for $\hat{\Phi}$ if s and h are sufficiently small:

$$(4.35) 1 + \hat{\Phi} \ge \epsilon_0^* := \frac{\epsilon_0}{2}, \quad 1 - \hat{\Phi} \ge \epsilon_0^*.$$

Such a uniform bound will be used in the convergence analysis.

In addition, since the correction function is only based on the projection solution (Φ_N, U_N, P_N) with enough regularity, its discrete $W_h^{1,\infty}$ norm will stay bounded: (4.36)

$$\|\hat{\Phi}^k\|_{\infty} \leq C^{\star}, \quad \|\hat{\boldsymbol{U}}^k\|_{\infty} \leq C^{\star}, \quad \|\nabla_h \hat{\Phi}^k\|_{\infty} \leq C^{\star}, \quad \|\nabla_h \hat{\boldsymbol{U}}^k\|_{\infty} \leq C^{\star}, \quad \forall k \geq 0.$$

4.2. **Rough error estimate.** Instead of a direct analysis for the error function (4.6), we introduce the perturbed numerical error function with second order truncation error:

$$(4.37) \quad \tilde{\phi}^n := \mathcal{P}_b \hat{\Phi}^n - \phi^n, \quad \tilde{\boldsymbol{u}}^n := \mathcal{P}_b \hat{\boldsymbol{U}}^n - \boldsymbol{u}^n, \quad \tilde{p}^n := \mathcal{P}_b \hat{P}^n - p^n, \quad \forall \ m \in \mathbb{N}.$$

In turn, subtracting the numerical scheme (3.1)-(3.4) from (4.27)-(4.30) gives

(4.38)
$$\frac{\tilde{\phi}^{n+1} - \tilde{\phi}^{n}}{s} = \Delta_{h} \tilde{\mu}^{n+1} - \nabla_{h} \cdot (A_{h} \tilde{\phi}^{n} \hat{\boldsymbol{U}}^{n+1} + A_{h} \phi^{n} \tilde{\boldsymbol{u}}^{n+1}) + \tau_{\phi}^{n+1},$$
$$\tilde{\mu}^{n+1} = \ln(1 + \hat{\phi}^{n+1}) - \ln(1 + \phi^{n+1}) - \ln(1 - \hat{\phi}^{n+1}) + \ln(1 - \phi^{n+1})$$

$$(4.39) -\theta_0 \tilde{\phi}^n - \varepsilon^2 \Delta_h \tilde{\phi}^{n+1},$$

(4.40)

$$(-\Delta_h + I)\tilde{\boldsymbol{u}}^{n+1} = -\nabla_h \tilde{\boldsymbol{p}}^{n+1} - \gamma (A_h \phi^n \nabla_h \tilde{\boldsymbol{\mu}}^{n+1} + A_h \tilde{\phi}^n \nabla_h \hat{\boldsymbol{\mathcal{V}}}^{n+1}) + \tau_v^{n+1},$$

$$(4.41) \quad \nabla_h \cdot \tilde{\boldsymbol{u}}^{n+1} = 0,$$

where

$$\|\tau_{\phi}^{n+1}\|_{2}, \|\tau_{v}^{n+1}\|_{2} \leq O(s^{2} + h^{2}).$$

Since $\hat{\mathcal{V}}^{n+1}$ only depends on the exact solution and correction function, we assume a discrete $W_h^{1,\infty}$ bound

In addition, we make the following a-priori assumption for the previous time step

Such an a-priori assumption will be recovered by the convergence analysis in the next time step, which will be demonstrated later. In turn, this a-priori assumption leads to an ℓ^{∞} bound, based on the inverse inequality and the linear refinement requirement $C_1h \leq s \leq C_2h$:

Lemma 4.1 states the rough error estimate; the detailed proof will be provided in Appendix A.

Lemma 4.1. We make the regularity assumption of \hat{V}^{n+1} (4.42), as well as the a-priori assumption (4.43). For the numerical error evolutionary system (4.38) – (4.41), a rough error estimate is valid:

As a direct consequence of the rough error estimate (4.45), an application of 3-D inverse inequality, combined with a discrete Sobolev inequality (given by (2.2)) in Lemma (2.2), reveals that

Furthermore, a combination of (4.46) and separation property (4.35) leads to a separation property of the numerical solution at the next time step t^{n+1}

(4.48)
$$\frac{\epsilon_0^*}{2} \le 1 + \phi^{n+1} \le 2, \quad \frac{\epsilon_0^*}{2} \le 1 - \phi^{n+1} \le 2.$$

Such a uniform bound will play a very important role in the refined error estimate.

Remark 4.3. It is noticed that the accuracy order in (4.45) is at least half order lower than the a-priori estimate (4.43), as well as the lower rate of the ℓ^{∞} error in (4.46), which comes from an application of the inverse inequality. In particular, the first order temporal truncation error is not sufficient to ensure the phase separation property; this is the reason why a complex process to construct higher order truncation error is needed. On the other hand, the a-priori assumption could not be covered by the lower accuracy rate in (4.45). Instead, such a separation property (4.48) will lead to a much sharper refined estimate.

4.3. Refined error estimate. Before proceeding into the refined error estimate, the following preliminary result for the nonlinear error term is needed. For simplicity of presentation, the detailed proof will be provided in Appendix B.

Lemma 4.2. Define

$$(4.49) \mathcal{L}^{n+1} = \ln(1 + \hat{\Phi}^{n+1}) - \ln(1 + \phi^{n+1}) - \ln(1 - \hat{\Phi}^{n+1}) + \ln(1 - \phi^{n+1}) - \theta_0 \tilde{\phi}^n.$$

Based on the separation property (4.48) for numerical solution, we have

$$(4.50) \|\nabla_h \mathcal{L}^{n+1}\|_2 \le 4(\epsilon_0^*)^{-1} \|\nabla_h \tilde{\phi}^{n+1}\|_2 + C(\epsilon_0^*)^{-2} \|\tilde{\phi}^{n+1}\|_4 + \theta_0 \|\nabla_h \tilde{\phi}^{n}\|_2.$$

Now we carry out the refined error estimate. Taking a discrete inner product with (4.38) by $-2\Delta_h \tilde{\phi}^{n+1}$ leads to

$$\frac{1}{s} \left(\|\nabla_{h} \tilde{\phi}^{n+1}\|_{2}^{2} - \|\nabla_{h} \tilde{\phi}^{n}\|_{2}^{2} + \|\nabla_{h} (\tilde{\phi}^{n+1} - \tilde{\phi}^{n})\|_{2}^{2} \right) + 2(\tilde{\boldsymbol{u}}^{n+1}, A_{h} \phi^{n} \nabla_{h} \Delta_{h} \tilde{\phi}^{n+1})$$

$$(4.51)$$

$$= 2(\nabla_{h} \tilde{\mu}^{n+1}, \nabla_{h} \Delta_{h} \tilde{\phi}^{n+1}) - 2(\tau_{\phi}^{n+1}, \Delta_{h} \tilde{\phi}^{n+1}) - 2(A_{h} \tilde{\phi}^{n} \hat{\boldsymbol{U}}^{n+1}, \nabla_{h} \Delta_{h} \tilde{\phi}^{n+1}),$$

where summation-by-parts formulas have been recalled. The Cauchy inequality could be applied to the local truncation error term:

$$(4.52) -2(\tau_{\phi}^{n+1}, \Delta_{h}\tilde{\phi}^{n+1}) \leq 2\|\tau_{\phi}^{n+1}\|_{-1,h} \cdot \|\nabla_{h}\Delta_{h}\tilde{\phi}^{n+1}\|_{2} \\ \leq 4\varepsilon^{-2}\|\tau_{\phi}^{n+1}\|_{-1,h}^{2} + \frac{\varepsilon^{2}}{4}\|\nabla_{h}\Delta_{h}\tilde{\phi}^{n+1}\|_{2}^{2}.$$

The third term on the right-hand-side could be bounded in a similar way

$$-2(A_{h}\tilde{\phi}^{n}\hat{\boldsymbol{U}}^{n+1}, \nabla_{h}\Delta_{h}\tilde{\phi}^{n+1}) \leq 2\|\hat{\boldsymbol{U}}^{n+1}\|_{\infty} \cdot \|\tilde{\phi}^{n}\|_{2} \cdot \|\nabla_{h}\Delta_{h}\tilde{\phi}^{n+1}\|_{2}$$

$$\leq 2C^{*}\|\tilde{\phi}^{n}\|_{2} \cdot \|\nabla_{h}\Delta_{h}\tilde{\phi}^{n+1}\|_{2}$$

$$\leq 4(C^{*})^{2}\varepsilon^{-2}\|\tilde{\phi}^{n}\|_{2}^{2} + \frac{\varepsilon^{2}}{4}\|\nabla_{h}\Delta_{h}\tilde{\phi}^{n+1}\|_{2}^{2}.$$

For the chemical potential diffusion term, the standard Cauchy inequality indicates that

$$(4.54) 2(\nabla_h \tilde{\mu}^{n+1}, \nabla_h \Delta_h \tilde{\phi}^{n+1}) = 2(\nabla_h \mathcal{L}^{n+1}, \nabla_h \Delta_h \tilde{\phi}^{n+1}) - 2\varepsilon^2 \|\nabla_h \Delta_h \tilde{\phi}^{n+1}\|_2^2$$

$$\leq 4\varepsilon^{-2} \|\nabla_h \mathcal{L}^{n+1}\|_2^2 - \frac{7\varepsilon^2}{4} \|\nabla_h \Delta_h \tilde{\phi}^{n+1}\|_2^2.$$

A similar estimate could be performed for the nonlinear convection error term

(4.55)
$$\nabla_{h} \Delta_{h} \tilde{\phi}^{n+1} = \varepsilon^{-2} (\nabla_{h} \mathcal{L}^{n+1} - \nabla_{h} \tilde{\mu}^{n+1}),$$

$$(\tilde{\boldsymbol{u}}^{n+1}, A_{h} \phi^{n} \nabla_{h} \mathcal{L}^{n+1}) \geq -\|\tilde{\boldsymbol{u}}^{n+1}\|_{2} \cdot \|\phi^{n}\|_{\infty} \cdot \|\nabla_{h} \mathcal{L}^{n+1}\|_{2}$$

$$(4.56) \geq -\|\tilde{\boldsymbol{u}}^{n+1}\|_{2} \cdot \|\nabla_{h} \mathcal{L}^{n+1}\|_{2} \geq -\frac{1}{4\gamma} \|\tilde{\boldsymbol{u}}^{n+1}\|_{2}^{2} - \gamma \|\nabla_{h} \mathcal{L}^{n+1}\|_{2}^{2}.$$

A combination with (A.6) gives

$$\begin{split} &2(\tilde{\boldsymbol{u}}^{n+1}, A_h \phi^n \nabla_h \Delta_h \tilde{\phi}^{n+1}) = 2\varepsilon^{-2} \left((\tilde{\boldsymbol{u}}^{n+1}, A_h \phi^n \nabla_h \mathcal{L}^{n+1}) - (\tilde{\boldsymbol{u}}^{n+1}, \mathcal{A}_h \phi^n \nabla_h \tilde{\mu}^{n+1}) \right) \\ &(4.57) \\ &\geq &2\varepsilon^{-2} \left(\frac{1}{2\gamma} \|\tilde{\boldsymbol{u}}^{n+1}\|_2^2 + \frac{1}{\gamma} \|\nabla_h \tilde{\boldsymbol{u}}^{n+1}\|_2^2 - \gamma \|\nabla_h \mathcal{L}^{n+1}\|_2^2 - \frac{2}{\gamma} \|\tau_v^{n+1}\|_2^2 - C \|\tilde{\phi}^n\|_2^2 \right). \end{split}$$

Substituting (4.52)–(4.54) and (4.57) into (4.51), combined with an application of Lemma (4.2), we obtain (4.58)

$$\begin{split} &\frac{1}{s} \left(\|\nabla_{h} \tilde{\phi}^{n+1}\|_{2}^{2} - \|\nabla_{h} \tilde{\phi}^{n}\|_{2}^{2} + \|\nabla_{h} (\tilde{\phi}^{n+1} - \tilde{\phi}^{n})\|_{2}^{2} \right) + \frac{5\varepsilon^{2}}{4} \|\nabla_{h} \Delta_{h} \tilde{\phi}^{n+1}\|_{2}^{2} \\ &+ \frac{\varepsilon^{-2}}{\gamma} (\|\tilde{\boldsymbol{u}}^{n+1}\|_{2}^{2} + 2\|\nabla_{h} \tilde{\boldsymbol{u}}^{n+1}\|_{2}^{2}) \\ &\leq 4\varepsilon^{-2} \left(\|\tau_{\phi}^{n+1}\|_{-1,h}^{2} + \|\tau_{v}^{n+1}\|_{2}^{2} \right) + 2\varepsilon^{-2} \left(2(C^{*})^{2} + C \right) \|\tilde{\phi}^{n}\|_{2}^{2} \\ &+ \varepsilon^{-2} (4 + 2\gamma) \|\nabla_{h} \mathcal{L}^{n+1}\|_{2}^{2} \\ &\leq 4\varepsilon^{-2} \left(\|\tau_{\phi}^{n+1}\|_{-1,h}^{2} + \|\tau_{v}^{n+1}\|_{2}^{2} \right) + 2\varepsilon^{-2} \left(2(C^{*})^{2} + C \right) \|\tilde{\phi}^{n}\|_{2}^{2} \\ &+ (12 + 6\gamma)\varepsilon^{-2} \left(16(\epsilon_{0}^{*})^{-2} \|\nabla_{h} \tilde{\phi}^{n+1}\|_{2}^{2} + C(\epsilon_{0}^{*})^{-4} \|\tilde{\phi}^{n+1}\|_{4}^{2} + \theta_{0}^{2} \|\nabla_{h} \tilde{\phi}^{n}\|_{2}^{2} \right) \\ &\leq 4\varepsilon^{-2} \left(\|\tau_{\phi}^{n+1}\|_{-1,h}^{2} + \|\tau_{v}^{n+1}\|_{2}^{2} \right) + 2C\varepsilon^{-2} \left(2(C^{*})^{2} + C \right) \|\nabla_{h} \tilde{\phi}^{n}\|_{2}^{2} \\ &+ (12 + 6\gamma)\varepsilon^{-2} \left(\left(16(\epsilon_{0}^{*})^{-2} + C(\epsilon_{0}^{*})^{-4} \right) \|\nabla_{h} \tilde{\phi}^{n+1}\|_{2}^{2} + \theta_{0}^{2} \|\nabla_{h} \tilde{\phi}^{n}\|_{2}^{2} \right), \end{split}$$

where the 3-D discrete Sobolev inequality, $\|\cdot\|_4 \leq C\|\cdot\|_{H_h^1}$ (given by (2.2) in Lemma 2.2), and the discrete Poincaré inequality have been used in last step.

Therefore, with sufficiently small s and h, an application of discrete Gronwall inequality leads to the desired higher order convergence estimate

(4.59)
$$\|\nabla_h \tilde{\phi}^{n+1}\|_2 + \left(\varepsilon^2 s \sum_{k=1}^{n+1} \|\nabla_h \Delta_h \tilde{\phi}^k\|_2^2\right)^{1/2} \le C(s^2 + h^2),$$

based on the higher order truncation error accuracy, $\|\tau_{\phi}^{n+1}\|_{-1,h}$, $\|\tau_{v}^{n+1}\|_{2} \leq C(s^{2} + h^{2})$. This completes the refined error estimate.

With the higher order convergence estimate (4.59) in hand, the a-priori assumption in (4.43) is recovered at the next time step t^{n+1} :

provided that s and h are sufficiently small, in which a discrete Poincaré inequality has been used again. Therefore, an induction analysis could be applied. This finishes the higher order convergence analysis.

As a result, the error estimate (4.7) for variable ϕ is a direct consequence of (4.60), combined with the boundedness of supplementary fields $\Phi_{\Delta t}$, as well as the projection approximation (4.3). This completes the proof of Theorem 4.1

Remark 4.4. In the Cahn-Hilliard-Stokes system (LLL)—(LA), a static Stokes equation is included. In other words, the velocity vector is statically determined by the phase variable and the chemical potential, combined with a Holmholtz projection into the divergence-free vector field. Meanwhile, many physical models are involved with time-dependent Stokes equation or Navier-Stokes equation, in which the temporal derivative of the velocity vector has to be taken into consideration. For the associated PDE system with temporal evolution of the velocity vector, the numerical scheme could be designed and analyzed in a similar fashion. The optimal rate convergence analysis could be theoretically established for the corresponding numerical schemes, following similar ideas presented in this article. The details are left to the future works.

5. Numerical experiments

In this section, we present a few numerical results, including a convergence test and some sample computations in a 2-D domain. The theoretical analysis is valid for both the 2-D and 3-D models, while we choose the 2-D domain in the numerical experiment, for simplicity in the implementation effort. The computational code for a 3-D domain could be similarly designed. A full approximation storage (FAS) nonlinear multigrid method is used to solve the nonlinear equations in the numerical scheme (3.1)–(3.4). See [9] for details about a similar solver. The first example demonstrates the robustness of the multigrid solver. The phase decomposition phenomenon, as well as the energy stability and mass conservation property of the proposed numerical scheme, will be verified in details. In another experiment we test the convergence order of the numerical scheme (3.1)–(3.4). The computational domain is taken as $\Omega = (0,1)^2$, and the physical parameters are set as: $\theta_0 = 3, \gamma = 1.0$. See [8] for comparison.

5.1. Spinodal decomposition, energy decay and mass conservation. In this subsection, we choose random initial data to display the phase decomposition phenomenon, energy decay and mass conservation. We set $\varepsilon = 0.01$, $h = \frac{1}{128}$,

 $s = 2 * 10^{-5}$ and initial data as

$$\phi_{i,j} = 0.2 + 0.02 * r_{i,j},$$

where $r_{i,j}$ is a random field of values that are uniformly distributed in [-1,1]. Figure \square describes evolution of the phase variable at some selected time levels with the initial condition (5.1). In addition, the associated maximum and minimum of the phase variable are given in Table \square

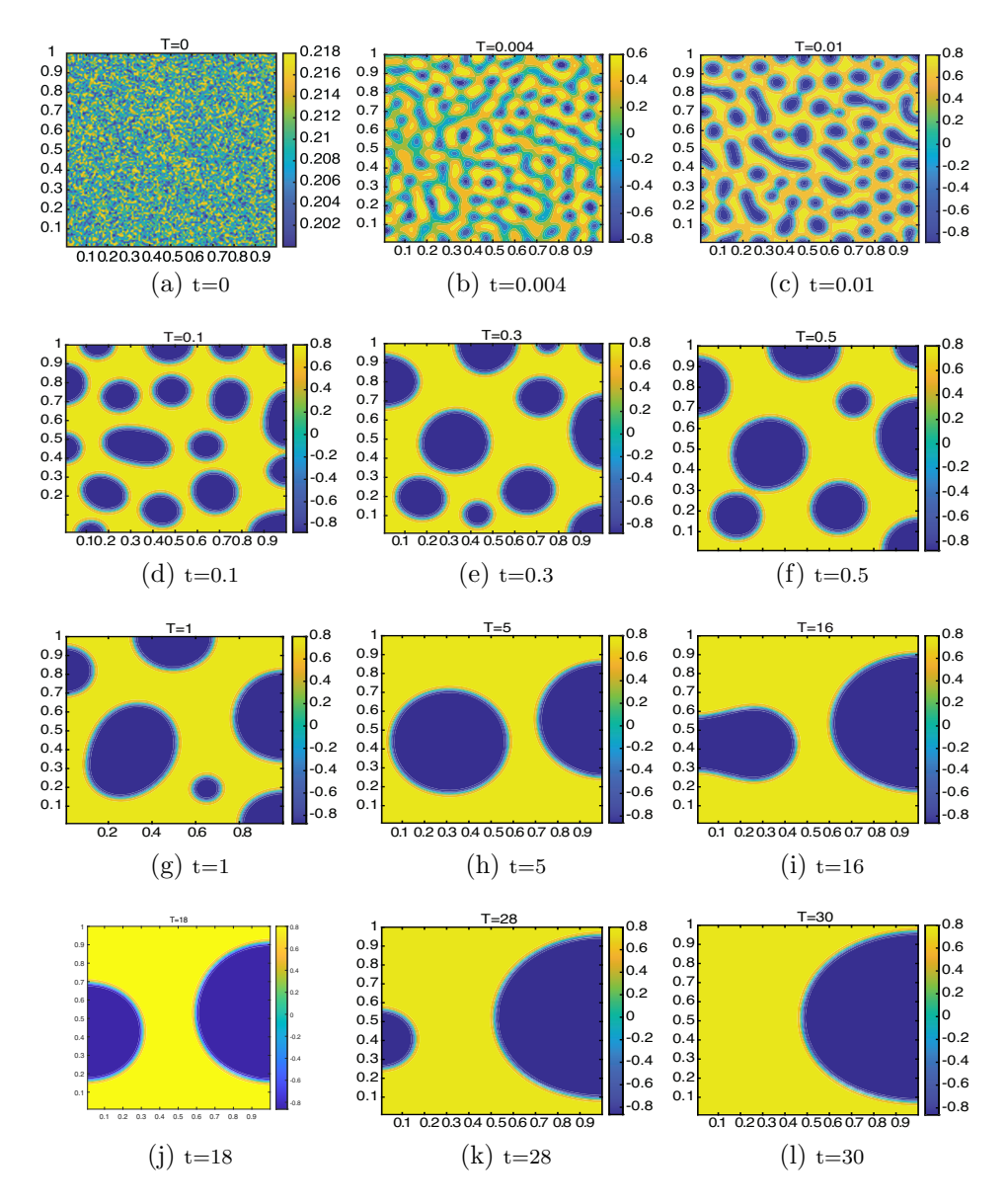


FIGURE 1. Evolution of the phase variable at selected times, with initial condition (5.1). Yellow corresponds to $\phi \approx 0.8$ and blue corresponds to $\phi \approx -0.8$.

For the system with polynomial energy functional (I.S), relevant numerical experiments have shown that concentration variable ϕ can overshoot the values ± 1 (I.S). Meanwhile, an obvious distance between the phase variable extrema and the singular limit values ± 1 is observed in Figure (I) and Table (I), which confirms the phase separation property. This numerical result gives a clear evidence that the singular logarithmic energy potential model leads to a much more powerful phase separation property than the polynomial approximation one.

Table 1.	The maximum	and minimum	values of t	he phase vari-
able at sele	ected time insta	ints, with initia	al condition	(5.1)

t	0	0.004	0.01	0.1	0.3	0.5
minimum	0.2000	-0.8147	-0.8772	-0.8732	-0.8759	-0.8713
maximum	0.2200	0.7934	0.8692	0.8527	0.8529	0.8524
t	1	5	16	18	28	30
minimum	-0.8731	-0.8623	-0.8629	-0.8624	-0.8647	-0.8610
maximum	0.8556	0.8551	0.8595	0.8562	0.8567	0.8570

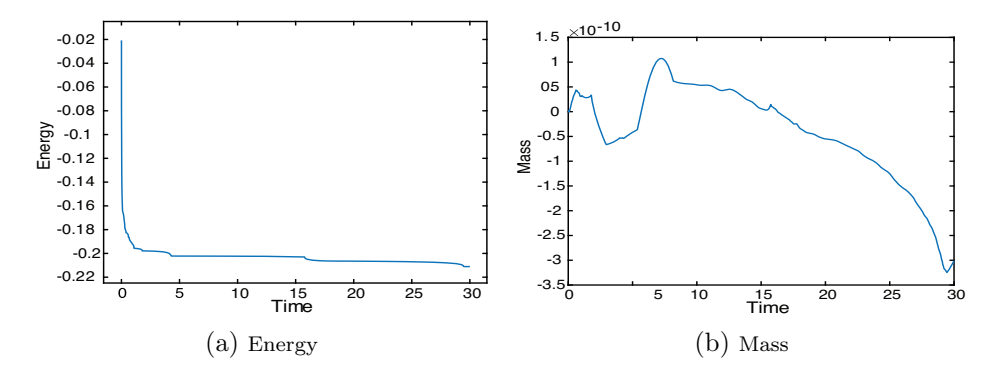


FIGURE 2. Energy decay and mass conservation with random initial condition (5.1)

The left plot of Figure 2 illustrates the evolution of discrete energy in terms of time, which confirms the energy dissipation property. The rough estimate of the mass difference computed as $\bar{\phi}^n - \bar{\phi}^0$ is displayed in the right plot of Figure 2, which numerically verifies the mass conservation property up to a machine error.

In addition, similar computations have been performed with trigonometric initial conditions,

(5.2)
$$\phi^0 = 0.9 * \left(\frac{(1 - \cos(4\pi x))(1 - \cos(4\pi y))}{2} - 1 \right),$$

the bound for which is adjusted to make the logarithmic energy meaningful. Parameters are the same as the last numerical test with random initial condition (5.1). Evolution of ϕ at selected time instants is displayed in Figure 3. Numerical verifications of energy dissipation and mass conservation are presented in Figure 4.

It is observed that the concentration variable ϕ stays stable, barely changing for a very long time. The same is true for the free energy. The left plot of Figure \Box

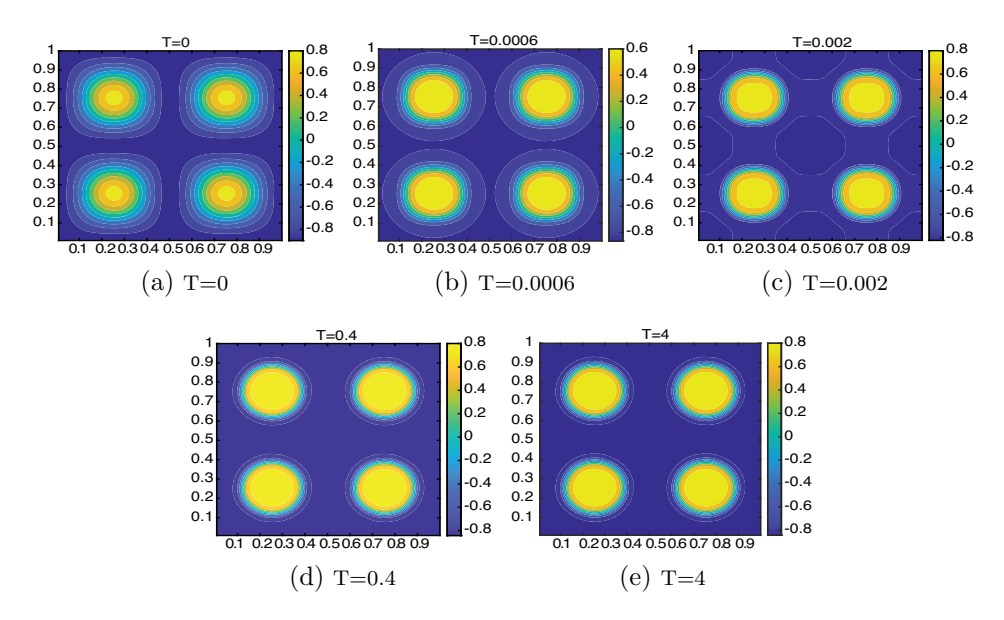


FIGURE 3. Evolution of the phase variable at selected time instants with trigonometric condition (5.2)

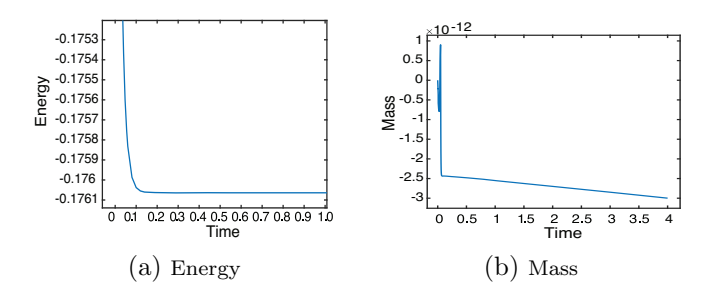


FIGURE 4. Test of energy decay and mass conservation with trigonometric initial condition (5.2)

illustrates the energy evolution from t = 0 to t = 0.1, since there is an extremely sharp decline in this range. However, the free energy is dissipated up to t = 4.

5.2. Convergence order. Now we present a convergence test for the numerical scheme (3.1)–(3.4), as $s, h \to 0$. Smooth initial data is taken via

(5.3)
$$\phi^0 = 0.24 * \cos(2\pi x) \cos(2\pi y) + 0.4 * \cos(\pi x) \cos(3\pi y).$$

The diffuse interface coefficient is set to $\varepsilon = 0.05$. We expect that the global error is of order $e_{t=T} = O(s) + O(h^2)$. In turn, with a refinement path $s = Ch^2$, we see that $e_{t=T} = O(h^2)$. In practice, we set $s = 0.02h^2$, the tolerant error for the FAS approach is set as $\tau = 10^{-8}$ and the final time is given by T = 0.02. Considering the multiple grid size and the definition of the cell-center function, the following

error expression is proposed:

(5.4)
$$e_{i,j}^{h-h/2} = \phi_{i,j}^h - \frac{1}{4} \left(\phi_{2i,2j}^{h/2} + \phi_{2i-1,2j}^{h/2} + \phi_{2i,2j-1)}^{h/2} + \phi_{2i-1,2j-1}^{h/2} \right).$$

The results are displayed in Table 2, which confirms the second order accuracy in space, as well as the first order accuracy in time.

Table 2. Numerical convergence test with initial data (5.2)

Grid size	$16^2 - 32^2$	$32^2 - 64^2$	$64^2 - 128^2$	$128^2 - 256^2$
L^2 error	1.9287E-02	4.5851E-03	1.1269E-03	2.8061E-04
. L^2 rate		2.0727	2.0245	2.0057
L^{∞} error	5.1703E- 02	1.1344E-02	2.9196E-03	7.3025E- 05
L^{∞} rate		2.1882	1.9581	1.9993

6. Conclusions

In this paper, we have presented a fully discrete finite difference numerical scheme of the Cahn-Hilliard-Stokes (CHS) system with Florry-Huggins energy potential. A convex splitting technique is applied to treat the chemical potential, combined with a semi-implicit computation of the nonlinear convection term, and an implicit update of the static Stokes equation. An implicit treatment of the logarithmic term ensures the positivity-preserving property, which comes from its singular nature as the phase variable approaches the singular limit values. An unconditional energy stability is derived by a careful energy estimate. Moreover, an optimal rate convergence analysis and error estimate has been established at a theoretical level, with the help of higher order consistency analysis, combined with rough and refined error (RRE) estimates. Some numerical experiments have also been presented, which demonstrate the theoretical properties of the proposed numerical scheme.

Appendix A. Proof of Lemma 4.1

Taking a discrete inner product with (4.38) by $\tilde{\mu}^{n+1}$ leads to

(A.1)
$$\frac{1}{s}(\tilde{\phi}^{n+1}, \tilde{\mu}^{n+1}) + \|\nabla_h \tilde{\mu}^{n+1}\|_2^2 - (A_h \phi^n \nabla_h \tilde{\mu}^{n+1}, \tilde{\boldsymbol{u}}^{n+1}) \\
= (A_h \tilde{\phi}^n \hat{\boldsymbol{U}}^{n+1}, \nabla_h \tilde{\mu}^{n+1}) + (\tau_{\phi}^{n+1}, \tilde{\mu}^{n+1}) + \frac{1}{s}(\tilde{\phi}^n, \tilde{\mu}^{n+1}).$$

Based on the mean-free property (4.34) of truncation error, the following estimate could be obtained

(A.2)
$$(\tau_{\phi}^{n+1}, \tilde{\mu}^{n+1}) \le \|\tau_{\phi}^{n+1}\|_{-1,h} \cdot \|\nabla_{h}\tilde{\mu}^{n+1}\|_{2} \le 2\|\tau_{\phi}^{n+1}\|_{-1,h}^{2} + \frac{1}{8}\|\nabla_{h}\tilde{\mu}^{n+1}\|_{2}^{2}.$$

For the $(\tilde{\phi}^n, \tilde{\mu}^{n+1})$ term, a similar analysis is valid

(A.3)
$$\frac{1}{s}(\tilde{\phi}^n, \tilde{\mu}^{n+1}) \le \frac{1}{s} \|\tilde{\phi}^n\|_{-1,h} \cdot \|\nabla_h \tilde{\mu}^{n+1}\|_2 \le \frac{2}{s^2} \|\tilde{\phi}^n\|_{-1,h}^2 + \frac{1}{8} \|\nabla_h \tilde{\mu}^{n+1}\|_2^2.$$

For the first term of right hand of (A.1), we see that (A.4)

$$(A_{h}\tilde{\phi}^{n}\hat{\boldsymbol{U}}^{n+1}, \nabla_{h}\tilde{\mu}^{n+1}) \leq \|\hat{\boldsymbol{U}}^{n+1}\|_{\infty} \cdot \|\tilde{\phi}^{n}\|_{2} \cdot \|\nabla_{h}\tilde{\mu}^{n+1}\|_{2} \leq C^{*}\|\tilde{\phi}^{n}\|_{2} \cdot \|\nabla_{h}\tilde{\mu}^{n+1}\|_{2}$$

$$\leq 2(C^{*})^{2}\|\tilde{\phi}^{n}\|_{2}^{2} + \frac{1}{8}\|\nabla_{h}\tilde{\mu}^{n+1}\|_{2}^{2}.$$

For the last term of right hand of (A.1), we begin with the following identity

$$(A.5) -A_h \phi^n \nabla_h \tilde{\mu}^{n+1} = \frac{1}{\gamma} \left((-\Delta_h + I) \tilde{\boldsymbol{u}}^{n+1} + \nabla_h \tilde{p}^{n+1} - \tau_v^{n+1} \right) + A_h \tilde{\phi}^n \nabla_h \hat{\mathcal{V}}^{n+1},$$

so that the following estimates are available

$$-(A_h\phi^n\nabla_h\tilde{\mu}^{n+1},\tilde{\boldsymbol{u}}^{n+1})$$

$$\begin{split} &= \left(\frac{1}{\gamma}(\tilde{\boldsymbol{u}}^{n+1} - \Delta_h \tilde{\boldsymbol{u}}^{n+1} + \nabla_h \tilde{p}^{n+1} - \tau_v^{n+1}) + A_h \tilde{\phi}^n \nabla_h \hat{\mathcal{V}}^{n+1}, \tilde{\boldsymbol{u}}^{n+1}\right) \\ &= \frac{1}{\gamma} \|\tilde{\boldsymbol{u}}^{n+1}\|_2^2 + \frac{1}{\gamma} \|\nabla_h \tilde{\boldsymbol{u}}^{n+1}\|_2^2 - \frac{1}{\gamma} (\tau_v^{n+1}, \tilde{\boldsymbol{u}}^{n+1}) + (A_h \tilde{\phi}^n \nabla_h \hat{\mathcal{V}}^{n+1}, \tilde{\boldsymbol{u}}^{n+1}) \\ &\geq \frac{1}{\gamma} \|\tilde{\boldsymbol{u}}^{n+1}\|_2^2 + \frac{1}{\gamma} \|\nabla_h \tilde{\boldsymbol{u}}^{n+1}\|_2^2 - \frac{1}{\gamma} \|\tau_v^{n+1}\|_2 \cdot \|\tilde{\boldsymbol{u}}^{n+1}\|_2 - \|\nabla_h \hat{\mathcal{V}}^{n+1}\|_{\infty} \cdot \|\tilde{\phi}^n\|_2 \cdot \|\tilde{\boldsymbol{u}}^{n+1}\|_2 \\ &\geq \frac{1}{\gamma} \|\tilde{\boldsymbol{u}}^{n+1}\|_2^2 + \frac{1}{\gamma} \|\nabla_h \tilde{\boldsymbol{u}}^{n+1}\|_2^2 - \frac{2}{\gamma} \|\tau_v^{n+1}\|_2^2 - \frac{1}{8\gamma} \|\tilde{\boldsymbol{u}}^{n+1}\|_2^2 - C \|\tilde{\phi}^n\|_2^2 - \frac{1}{8\gamma} \|\tilde{\boldsymbol{u}}^{n+1}\|_2^2 \\ &\geq \frac{3}{4\gamma} \|\tilde{\boldsymbol{u}}^{n+1}\|_2^2 + \frac{1}{\gamma} \|\nabla_h \tilde{\boldsymbol{u}}^{n+1}\|_2^2 - \frac{2}{\gamma} \|\tau_v^{n+1}\|_2^2 - C \|\tilde{\phi}^n\|_2^2. \end{split}$$

Meanwhile, an application of intermediate value theorem implies a point-wise representation:

(A.7)

$$\ln(1+\hat{\Phi}^{n+1}) - \ln(1+\phi^{n+1}) = \frac{\tilde{\phi}^{n+1}}{1+\eta^{(n+1)}}, \quad \eta^{(n+1)} \text{ is between } \phi^{n+1} \text{ and } \hat{\Phi}^{n+1}.$$

By the point-wise bound that $-1 < \phi^{n+1}$, $\hat{\Phi}^{n+1} < 1$, we have $0 < 1 + \eta^{(n+1)} < 2$ so that $\frac{1}{1+\eta^{(n+1)}} > \frac{1}{2}$,

(A.8)
$$(\ln(1+\hat{\Phi}^{n+1}) - \ln(1+\phi^{n+1}), \tilde{\phi}^{n+1}) = (\frac{\tilde{\phi}^{n+1}}{1+\eta^{(n+1)}}, \tilde{\phi}^{n+1}) \ge \frac{1}{2} \|\tilde{\phi}^{n+1}\|_2^2$$

A similar analysis could be derived:

(A.9)
$$(-\ln(1-\hat{\Phi}^{n+1}) + \ln(1-\phi^{n+1}), \tilde{\phi}^{n+1}) \ge \frac{1}{2} \|\tilde{\phi}^{n+1}\|_2^2.$$

The two linear terms in the expansion of $(\tilde{\phi}^{n+1}, \tilde{\mu}^{n+1})$ could be analyzed in a more straightforward way:

(A.10)
$$-\theta_0(\tilde{\phi}^n, \tilde{\phi}^{n+1}) \ge -\frac{1}{2}\theta_0^2 \|\tilde{\phi}^n\|_2^2 - \frac{1}{2}\|\tilde{\phi}^{n+1}\|_2^2,$$

(A.11)
$$-(\Delta_h \tilde{\phi}^{n+1}, \tilde{\phi}^{n+1}) = \|\nabla_h \tilde{\phi}^{n+1}\|_{2}^{2}.$$

Then we conclude that

(A.12)
$$(\tilde{\phi}^{n+1}, \tilde{\mu}^{n+1}) \ge \frac{1}{2} \|\tilde{\phi}^{n+1}\|_2^2 + \frac{\varepsilon^2}{2} \|\nabla_h \tilde{\phi}^{n+1}\|_2^2 - \frac{\theta_0^2}{2} \|\tilde{\phi}^n\|_2^2.$$

A substitution of (A.1)–(A.4), (A.6) and (A.12) shows that (A.13)

$$\frac{1}{2} \|\tilde{\phi}^{n+1}\|_{2}^{2} + \frac{\varepsilon^{2}}{2} \|\nabla_{h}\tilde{\phi}^{n+1}\|_{2}^{2} + s(\frac{5}{8} \|\nabla_{h}\tilde{\mu}^{n+1}\|_{2}^{2} + \frac{3}{4\gamma} \|\tilde{\boldsymbol{u}}^{n+1}\|_{2}^{2} + \frac{1}{\gamma} \|\nabla_{h}\tilde{\boldsymbol{u}}^{n+1}\|_{2}^{2})$$

$$\leq \frac{2}{s} \|\tilde{\phi}^{n}\|_{-1,h}^{2} + C \|\tilde{\phi}^{n}\|_{2}^{2} + s(\frac{2}{\gamma} \|\tau_{v}^{n+1}\|_{2}^{2} + 2 \|\tau_{\phi}^{n+1}\|_{-1,h}^{2}).$$

For the right hand side of (A.13), the following estimates are available, which come from the a-priori assumption (4.43):

$$(A.14) \qquad \frac{2}{s} \|\tilde{\phi}^n\|_{-1,h}^2 \le \frac{C}{s} \|\tilde{\phi}^n\|_2^2 \le C(s^{\frac{11}{4}} + h^{\frac{11}{4}}),$$

$$C\|\tilde{\phi}^n\|_2^2 \le C(s^{\frac{15}{4}} + h^{\frac{15}{4}}),$$

$$s(\frac{2}{\gamma} \|\tau_v^{n+1}\|_2^2 + 2\|\tau_\phi^{n+1}\|_{-1,h}^2) \le C(s^5 + h^5),$$

where the fact that $||f||_{-1,h} \le C||f||_2$, as well as the refinement constraint $C_1h \le s \le C_2h$, has been repeatedly used. Going back to (A.13), we have

(A.15)
$$\|\tilde{\phi}^{n+1}\|_{2} + \|\nabla_{h}\tilde{\phi}^{n+1}\|_{2} \le C(s^{\frac{11}{8}} + h^{\frac{11}{8}}) \le \hat{C}(s^{\frac{5}{4}} + h^{\frac{5}{4}}),$$

under the linear refinement requirement $C_1h \leq s \leq C_2h$, provided that s and h are sufficiently small. In addition, \hat{C} depends on the physical parameters, while it is independent of s and h. This inequality is exactly the rough error estimate (4.45). The proof of Lemma 4.1 is complete.

APPENDIX B. PROOF OF LEMMA 4.2

We focus on the nonlinear term $\ln(1+\hat{\Phi}^{n+1})-\ln(1+\phi^{n+1})$. The other terms could be similarly analyzed. The decomposition identity (A.7) is still valid. Considering a single mesh cell, we make the following observation

$$D_{x}(\ln(1+\hat{\Phi}^{n+1}) - \ln(1+\phi^{n+1}))_{i+\frac{1}{2},j,k} = D_{x}(\frac{1}{1+\eta^{(n+1)}} \cdot \tilde{\phi}^{n+1})_{i+\frac{1}{2},j,k}$$

$$=: \mathcal{NLE}_{1} + \mathcal{NLE}_{2},$$

$$\mathcal{NLE}_{1} = \frac{1}{1+\eta^{(n+1)}_{i+1,j,k}} D_{x} \tilde{\phi}^{n+1}_{i+\frac{1}{2},j,k}, \quad \mathcal{NLE}_{2} = \tilde{\phi}^{n+1}_{i,j,k} D_{x}(\frac{1}{1+\eta^{(n+1)}})_{i+\frac{1}{2},j,k}.$$

The bound for the first nonlinear expansion is straightforward:

(B.2)
$$0 < \frac{1}{1 + \eta_{i+1, j, k}^{(n+1)}} \le (\frac{1}{2} \epsilon_0^*)^{-1} = 2(\epsilon_0^*)^{-1}, \text{ (by (4.35), (4.48))},$$

(B.3) so that
$$\|\frac{1}{1+\eta^{(n+1)}}\|_{\infty} \le 2(\epsilon_0^*)^{-1}$$
,

(B.4)
$$\|\mathcal{NLE}_1\|_2 \le \|\frac{1}{1+n^{(n+1)}}\|_{\infty} \cdot \|D_x\tilde{\phi}^{n+1}\|_2 \le 2(\epsilon_0^*)^{-1}\|D_x\tilde{\phi}^{n+1}\|_2.$$

Meanwhile, by the decomposition identity (A.7), we denote

(B.5)
$$e_{i,j,k} = \hat{\Phi}_{i,j,k}^{n+1} - \eta_{i,j,k}^{(n+1)}.$$

It is clear that

(B.6)
$$|e_{i,j,k}| \le |\hat{\Phi}_{i,j,k}^{n+1} - \phi_{i,j,k}^{n+1}| = |\tilde{\phi}_{i,j,k}^{n+1}|, \quad \forall (i,j,k).$$

By the discrete $\|\cdot\|_4$ rough estimation (4.47), an application of inverse inequality gives

(B.7)
$$\|\nabla_h e\|_4 \le \frac{C\|e\|_4}{h} \le \frac{C\|\tilde{\phi}^{n+1}\|_4}{h} \le \frac{C(s^{\frac{5}{4}} + h^{\frac{5}{4}})}{h} \le C(s^{\frac{1}{4}} + h^{\frac{1}{4}}) \le \frac{1}{2},$$

under the linear refinement requirement $C_1h \leq s \leq C_2h$, provided that s and h are sufficiently small. In turn, we see that

(B.8)
$$(D_x \eta^{(n+1)})_{i+\frac{1}{2},j,k} = (D_x \hat{\Phi}^{n+1})_{i+\frac{1}{2},j,k} - (D_x e)_{i+\frac{1}{2},j,k},$$

$$||D_x \eta^{(n+1)}||_4 \le ||D_x \hat{\Phi}^{n+1}||_4 + ||D_x e||_4 \le C^* + \frac{1}{2}.$$

On the other hand, motivated by the following expansion

(B.9)
$$D_x(\frac{1}{1+\eta^{(n+1)}})_{i+\frac{1}{2},j,k} = \frac{-(D_x\eta^{(n+1)})_{i+\frac{1}{2},j,k}}{(1+\eta^{n+1}_{i,j,k})(1+\eta^{n+1}_{i+1,j,k})},$$

we conclude that

(B.10)
$$||D_x(\frac{1}{1+\eta^{(n+1)}})||_4 \le \max_{i,j,k} \frac{1}{(1+\eta^{n+1}_{i,j,k})(1+\eta^{n+1}_{i+1,j,k})} \cdot ||D_x\eta^{(n+1)}||_4$$

$$\le 2(\epsilon_0^*)^{-2}(C^* + \frac{1}{2}),$$

in which the phase separation estimates (4.35) and (4.48) have been applied again. Then we arrive at

(B.11)
$$\|\mathcal{NLE}_2\|_2 \le \|D_x(\frac{1}{1+\eta^{(n+1)}})\|_4 \cdot \|\tilde{\phi}^{n+1}\|_4 \le 2(\epsilon_0^*)^{-2} \cdot C\|\tilde{\phi}^{n+1}\|_4.$$

Subsequently, a combination of (B.4) and (B.11) leads to (B.12)

$$\|D_x(\ln(1+\hat{\Phi}^{n+1})-\ln(1+\phi^{n+1}))\|_2 \le 2(\epsilon_0^*)^{-1}\|D_x\tilde{\phi}^{n+1}\|_2 + 2(\epsilon_0^*)^{-2}C\|\tilde{\phi}^{n+1}\|_4.$$

Similar estimates could be derived in the y and z directions; the technical details are skipped for the sake of brevity:

$$||D_y(\ln(1+\hat{\Phi}^{n+1}) - \ln(1+\phi^{n+1}))||_2 \le 2(\epsilon_0^*)^{-1}||D_y\tilde{\phi}^{n+1}||_2 + 2(\epsilon_0^*)^{-2}C||\tilde{\phi}^{n+1}||_4,$$
(B.14)

$$||D_z(\ln(1+\hat{\Phi}^{n+1})-\ln(1+\phi^{n+1}))||_2 \le 2(\epsilon_0^*)^{-1}||D_z\tilde{\phi}^{n+1}||_2 + 2(\epsilon_0^*)^{-2}C||\tilde{\phi}^{n+1}||_4.$$

Therefore, a combination of (B.12)–(B.14) yields (B.15)

$$\|\nabla_h(\ln(1+\hat{\Phi}^{n+1}) - \ln(1+\phi^{n+1}))\|_2 \le 2(\epsilon_0^*)^{-1} \|\nabla_h\tilde{\phi}^{n+1}\|_2 + 2\sqrt{3}(\epsilon_0^*)^{-2}C\|\tilde{\phi}^{n+1}\|_4.$$

A similar estimate could also be derived for the error term of $-\ln(1-\hat{\Phi}^{n+1}) + \ln(1-\phi^{n+1})$:

$$\|\nabla_h(-\ln(1-\hat{\Phi}^{n+1})+\ln(1-\phi^{n+1}))\|_2 \le 2(\epsilon_0^*)^{-1}\|\nabla_h\tilde{\phi}^{n+1}\|_2 + 2\sqrt{3}(\epsilon_0^*)^{-2}C\|\tilde{\phi}^{n+1}\|_4.$$

Finally, a substitution of (B.15) and (B.16) into the nonlinear error expansion (4.49) results in the desired estimate (4.50). This finishes the proof of Lemma 4.2.

ACKNOWLEDGMENT

Y. Z. Guo thanks the Hong Kong Polytechnic University for the generous support and hospitality during his visit.

References

- J. W. Barrett and J. F. Blowey, Finite element approximation of the Cahn-Hilliard equation with concentration dependent mobility, Math. Comp. 68 (1999), no. 226, 487–517, DOI 10.1090/S0025-5718-99-01015-7. MR 1609678
- [2] W. Chen, W. Feng, Y. Liu, C. Wang, and S. M. Wise, A second order energy stable scheme for the Cahn-Hilliard-Hele-Shaw equations, Discrete Contin. Dyn. Syst. Ser. B 24 (2019), no. 1, 149–182, DOI 10.3934/dcdsb.2018090. MR3932721
- [3] W. Chen, S. Wang, Y. Zhang, D. Han, C. Wang, and X. Wang, Error estimate of a decoupled numerical scheme for the Cahn-Hilliard-Stokes-Darcy system, IMA J. Numer. Anal. 42 (2022), no. 3, 2621–2655, DOI 10.1093/imanum/drab046. MR4454932
- [4] W. Chen, J. Jing, Q. Liu, C. Wang, and X. Wang, A second order accurate, positivity-preserving numerical scheme of the Cahn-Hilliard-Navier-Stokes system with Flory-Huggins potential, Commun. Comput. Phys., 2023. accepted and in press.
- [5] W. Chen, J. Jing, C. Wang, and X. Wang, A positivity preserving, energy stable finite difference scheme for the Flory-Huggins-Cahn-Hilliard-Navier-Stokes system, J. Sci. Comput. 92 (2022), no. 2, Paper No. 31, 24, DOI 10.1007/s10915-022-01872-1. MR4443516
- [6] W. Chen, J. Jing, C. Wang, X. Wang, and S. M. Wise, A modified Crank-Nicolson numerical scheme for the Flory-Huggins Cahn-Hilliard model, Commun. Comput. Phys. 31 (2022), no. 1, 60–93, DOI 10.4208/cicp.oa-2021-0074. MR4350698
- W. Chen, Y. Liu, C. Wang, and S. M. Wise, Convergence analysis of a fully discrete finite difference scheme for the Cahn-Hilliard-Hele-Shaw equation, Math. Comp. 85 (2016), no. 301, 2231–2257, DOI 10.1090/mcom3052. MR3511281
- W. Chen, C. Wang, X. Wang, and S. M. Wise, Positivity-preserving, energy stable numerical schemes for the Cahn-Hilliard equation with logarithmic potential, J. Comput. Phys. X 3 (2019), 100031, 29, DOI 10.1016/j.jcpx.2019.100031. MR4116082
- [9] C. Collins, J. Shen, and S. M. Wise, An efficient, energy stable scheme for the Cahn-Hilliard-Brinkman system, Commun. Comput. Phys. 13 (2013), no. 4, 929–957, DOI 10.4208/cicp.171211.130412a. MR2982944
- [10] F. Della Porta, A. Giorgini, and M. Grasselli, The nonlocal Cahn-Hilliard-Hele-Shaw system with logarithmic potential, Nonlinearity 31 (2018), no. 10, 4851–4881, DOI 10.1088/1361-6544/aad52a. MR3856121
- [11] A. E. Diegel, C. Wang, and S. M. Wise, Stability and convergence of a second-order mixed finite element method for the Cahn-Hilliard equation, IMA J. Numer. Anal. 36 (2016), no. 4, 1867–1897, DOI 10.1093/imanum/drv065. MR3556407
- [12] A. E. Diegel, C. Wang, X. Wang, and S. M. Wise, Convergence analysis and error estimates for a second order accurate finite element method for the Cahn-Hilliard-Navier-Stokes system, Numer. Math. 137 (2017), no. 3, 495–534, DOI 10.1007/s00211-017-0887-5. MR3712284
- [13] L. Dong, C. Wang, S. M. Wise, and Z. Zhang, A positivity-preserving, energy stable scheme for a ternary Cahn-Hilliard system with the singular interfacial parameters, J. Comput. Phys. 442 (2021), Paper No. 110451, 29, DOI 10.1016/j.jcp.2021.110451. MR4270095
- [14] L. Dong, C. Wang, H. Zhang, and Z. Zhang, A positivity-preserving, energy stable and convergent numerical scheme for the Cahn-Hilliard equation with a Flory-Huggins-de-Gennes energy, Commun. Math. Sci. 17 (2019), no. 4, 921–939, DOI 10.4310/CMS.2019.v17.n4.a3. MR4030506
- [15] L. Dong, C. Wang, H. Zhang, and Z. Zhang, A positivity-preserving second-order BDF scheme for the Cahn-Hilliard equation with variable interfacial parameters, Commun. Comput. Phys. 28 (2020), no. 3, 967–998, DOI 10.4208/cicp.oa-2019-0037. MR4126520
- [16] C. Duan, W. Chen, C. Liu, C. Wang, and X. Yue, A second order accurate, energy stable numerical scheme for the one-dimensional porous medium equation by an energetic variational approach, Commun. Math. Sci. 20 (2022), no. 4, 987–1024, DOI 10.4310/CMS.2022.v20.n4.a3. MR4407510

- [17] C. Duan, W. Chen, C. Liu, C. Wang, and S. Zhou, Convergence analysis of structure-preserving numerical methods for nonlinear Fokker-Planck equations with nonlocal interactions, Math. Methods Appl. Sci. 45 (2022), no. 7, 3764–3781, DOI 10.1002/mma.8015. MR4407950
- [18] C. Duan, C. Liu, C. Wang, and X. Yue, Convergence analysis of a numerical scheme for the porous medium equation by an energetic variational approach, Numer. Math. Theory Methods Appl. 13 (2020), no. 1, 63–80, DOI 10.4208/nmtma.oa-2019-0073. MR4044415
- [19] D. Eyre, Unconditionally gradient stable time marching the Cahn-Hilliard equation, In J. W. Bullard, R. Kalia, M. Stoneham, and L.Q. Chen, editors, Computational and Mathematical Models of Microstructural Evolution, volume 53, pages 1686–1712, Warrendale, PA, USA, 1998. Materials Research Society.
- [20] X. Feng and S. Wise, Analysis of a Darcy-Cahn-Hilliard diffuse interface model for the Hele-Shaw flow and its fully discrete finite element approximation, SIAM J. Numer. Anal. 50 (2012), no. 3, 1320–1343, DOI 10.1137/110827119. MR2970745
- [21] Z. Guan, J. Lowengrub, and C. Wang, Convergence analysis for second-order accurate schemes for the periodic nonlocal Allen-Cahn and Cahn-Hilliard equations, Math. Methods Appl. Sci. 40 (2017), no. 18, 6836–6863, DOI 10.1002/mma.4497. MR3742100
- [22] Z. Guan, C. Wang, and S. M. Wise, A convergent convex splitting scheme for the periodic non-local Cahn-Hilliard equation, Numer. Math. 128 (2014), no. 2, 377–406, DOI 10.1007/s00211-014-0608-2. MR3259494
- [23] D. Han and X. Wang, A second order in time, uniquely solvable, unconditionally stable numerical scheme for Cahn-Hilliard-Navier-Stokes equation, J. Comput. Phys. 290 (2015), 139–156, DOI 10.1016/j.jcp.2015.02.046. MR3324579
- [24] Z. Hu, S. M. Wise, C. Wang, and J. S. Lowengrub, Stable and efficient finite-difference nonlinear-multigrid schemes for the phase field crystal equation, J. Comput. Phys. 228 (2009), no. 15, 5323–5339, DOI 10.1016/j.jcp.2009.04.020. MR2541456
- [25] H.-G. Lee, J. S. Lowengrub, and J. Goodman, Modeling pinchoff and reconnection in a Hele-Shaw cell. I. The models and their calibration, Phys. Fluids 14 (2002), no. 2, 492–513, DOI 10.1063/1.1425843. MR1878351
- [26] X. Li, Z. Qiao, and C. Wang, Double stabilizations and convergence analysis of a secondorder linear numerical scheme for the nonlocal Cahn-Hilliard equation, Sci. China Math., 2022. Accepted and in press.
- [27] X. Li, Z. Qiao, and C. Wang, Stabilization parameter analysis of a second-order linear numerical scheme for the nonlocal Cahn-Hilliard equation, IMA J. Numer. Anal. 43 (2023), no. 2, 1089–1114, DOI 10.1093/imanum/drab109. MR4568441
- [28] C. Liu, C. Wang, and Y. Wang, A structure-preserving, operator splitting scheme for reactiondiffusion equations with detailed balance, J. Comput. Phys. 436 (2021), Paper No. 110253, 22, DOI 10.1016/j.jcp.2021.110253. MR4234219
- [29] C. Liu, C. Wang, S. M. Wise, X. Yue, and S. Zhou, A positivity-preserving, energy stable and convergent numerical scheme for the Poisson-Nernst-Planck system, Math. Comp. 90 (2021), no. 331, 2071–2106, DOI 10.1090/mcom/3642. MR4280293
- [30] C. Liu, C. Wang, S. M. Wise, X. Yue, and S. Zhou, An iteration solver for the Poisson-Nernst-Planck system and its convergence analysis, J. Comput. Appl. Math. 406 (2022), Paper No. 114017, 13, DOI 10.1016/j.cam.2021.114017. MR4356837
- [31] Y. Liu, W. Chen, C. Wang, and S. M. Wise, Error analysis of a mixed finite element method for a Cahn-Hilliard-Hele-Shaw system, Numer. Math. 135 (2017), no. 3, 679–709, DOI 10.1007/s00211-016-0813-2. MR3606459
- [32] Y. Qian, C. Wang, and S. Zhou, A positive and energy stable numerical scheme for the Poisson-Nernst-Planck-Cahn-Hilliard equations with steric interactions, J. Comput. Phys. 426 (2021), Paper No. 109908, 17, DOI 10.1016/j.jcp.2020.109908. MR4195851
- [33] J. Shen, C. Wang, X. Wang, and S. M. Wise, Second-order convex splitting schemes for gradient flows with Ehrlich-Schwoebel type energy: application to thin film epitaxy, SIAM J. Numer. Anal. 50 (2012), no. 1, 105–125, DOI 10.1137/110822839. MR288306
- [34] J. Shen and X. Yang, Decoupled, energy stable schemes for phase-field models of two-phase incompressible flows, SIAM J. Numer. Anal. 53 (2015), no. 1, 279–296, DOI 10.1137/140971154. MR3303685

- [35] C. Wang and S. M. Wise, An energy stable and convergent finite-difference scheme for the modified phase field crystal equation, SIAM J. Numer. Anal. 49 (2011), no. 3, 945–969, DOI 10.1137/090752675. MR2802554
- [36] S. M. Wise, Unconditionally stable finite difference, nonlinear multigrid simulation of the Cahn-Hilliard-Hele-Shaw system of equations, J. Sci. Comput. 44 (2010), no. 1, 38–68, DOI 10.1007/s10915-010-9363-4. MR\u00e92647498
- [37] S. M. Wise, C. Wang, and J. S. Lowengrub, An energy-stable and convergent finite-difference scheme for the phase field crystal equation, SIAM J. Numer. Anal. 47 (2009), no. 3, 2269– 2288, DOI 10.1137/080738143. MR2519603
- [38] X. Yang and J. Zhao, On linear and unconditionally energy stable algorithms for variable mobility Cahn-Hilliard type equation with logarithmic Flory-Huggins potential, Commun. Comput. Phys. 25 (2019), no. 3, 703–728, DOI 10.4208/cicp.oa-2017-0259. MR3878519
- [39] M. Yuan, W. Chen, C. Wang, S. M. Wise, and Z. Zhang, An energy stable finite element scheme for the three-component Cahn-Hilliard-type model for macromolecular microsphere composite hydrogels, J. Sci. Comput. 87 (2021), no. 3, Paper No. 78, 30, DOI 10.1007/s10915-021-01508-w. MR4251690
- [40] J. Zhang, C. Wang, S. M. Wise, and Z. Zhang, Structure-preserving, energy stable numerical schemes for a liquid thin film coarsening model, SIAM J. Sci. Comput. 43 (2021), no. 2, A1248–A1272, DOI 10.1137/20M1375656. MR4241519

School of Mathematical Sciences, Beijing Normal University, Beijing 100875, People's Republic of China

 $Email\ address \hbox{: } \verb"yunzguo@mail.bnu.edu.cn"$

Department of Mathematics, The University of Massachusetts, North Dartmouth, Massachusetts 02747

Email address: cwang1@umassd.edu

Department of Mathematics, The University of Tennessee, Knoxville, Tennessee 37996

Email address: swise1@utk.edu

Laboratory of Mathematics and Complex Systems, Beijing Normal University, Beijing 100875, People's Republic of China

Email address: zrzhang@bnu.edu.cn